Original paper

Progressive gene dose-dependent disruption of the methamphetamine-sensitive circadian oscillator-driven rhythms in a knock-in mouse model of Huntington's disease

Koliane Ouk, Juliet Aungier and A. Jennifer Morton*

Department of Physiology, Development and Neuroscience, University of Cambridge, Cambridge, Downing Street, CB2 3DY, United Kingdom

E-mail addresses for all authors:

Koliane Ouk: ko303@cam.ac.uk

Juliet Aungier: ja448@cam.ac.uk

A. Jennifer Morton: ajm41@cam.ac.uk

*Corresponding author
Prof. Jenny Morton
E-mail address: ajm41@cam.ac.uk
Tel: +44 1223 334057
Fax: +44 1223 333840

Abstract

Huntington's disease (HD) is a progressive genetic neurodegenerative disorder characterised by motor and cognitive deficits, as well as sleep and circadian abnormalities. In the R6/2 mouse, a fragment model of HD, rest-activity rhythms controlled by the suprachiasmatic nucleus disintegrate completely by 4 months of age. Rhythms driven by a second circadian oscillator, the methamphetamine-sensitive circadian oscillator (MASCO), are disrupted even earlier, and cannot be induced after 2 months of age. Here, we studied the effect of the HD mutation on the expression of MASCO-driven rhythms in a more slowly developing, genetically relevant mouse model of HD, the Q175 'knock-in' mouse. We induced expression of MASCO output by administering low dose methamphetamine (0.005%) chronically via the drinking water. We measured locomotor activity in constant darkness in wild-type and Q175 mice at 2 (presymptomatic), 6 (early symptomatic), and 12 (symptomatic) months of age. At 2 months, all mice expressed MASCO-driven rhythms, regardless of genotype. At older ages, however, there was a progressive gene dose-dependent deficit in MASCO output in Q175 mice. At 6 months of age, these rhythms could be observed in only 45% of heterozygous and 15% of homozygous mice. By 1 year of age, 90% of homozygous mice had an impaired MASCO output. There was also an age-dependent disruption of MASCO output seen in wild-type mice. The fact that the progressive deficit in MASCO-driven rhythms in Q175 mice is HD gene dose-dependent suggests that, whatever its role in humans, abnormalities in MASCO output may contribute to the HD circadian phenotype.

1. Introduction

Huntington's disease (HD) is an inherited neurodegenerative condition caused by an unstable expansion of CAG repeats in the Huntingtin (*HTT*) gene. The age onset of HD is inversely correlated to CAG repeat length (The Huntington's Disease Collaborative Research group, 1993) and is similar in homozygous (HOM) and heterozygous (HET) patients, although HD progresses more rapidly in HOM (Squitieri et al., 2003). HD is characterised by a progressive decline in locomotor and cognitive functions (see Bates et al., 2015 for references). As well, abnormalities in circadian rhythmicity and sleep have been described in HD patients (Arnulf et al., 2008; Lazar et al., 2015; Morton, 2013; Morton et al., 2005; Piano et al., 2015). These are recapitulated in multiple HD mouse models (Fisher et al., 2016, 2013; Jeantet et al., 2013; Kantor et al., 2013; Kudo et al., 2011; Lebreton et al., 2015; Morton et al., 2005). The hemizygous R6/2 transgenic mouse is the best characterised of these models of HD (Carter et al., 1999; Mangiarini et al., 1996; Menalled et al., 2009; Morton et al., 2005; Pouladi et al., 2012). With a transgene carrying ~250 CAG repeats, the R6/2 mouse has a rapid progression of disease with disruption in circadian behaviours at ~12 weeks and a lifespan of ~22 weeks (Wood et al., 2013). It is not known however, how the gene mutation causes the circadian changes that occur in the R6/2 mouse.

Under normal physiological conditions, circadian rhythms are driven and coordinated by the suprachiasmatic nucleus of the hypothalamus (SCN). The SCN, however, is not the only oscillator that can regulate daily rhythms. For example, the methamphetamine-sensitive circadian oscillator (MASCO), is a putative circadian pacemaker that generates behavioural rhythms independent of the SCN (Honma et al., 1987, 1988). MASCO-dependent rhythms are induced by chronic low dose treatment of methamphetamine (MAP). When a chronic treatment with MAP is given to SCN-intact wild-type (WT) mice placed in constant darkness (DD), a dissociation of the circadian

locomotor activity rhythms can occur, leading to two rhythms, one component driven by the SCN (~24h) and a longer one driven by the MASCO (usually >24h; Cuesta et al., 2012; Honma et al., 1986; Tataroglu et al., 2006). The MASCO-driven rhythms are severely disrupted in R6/2 mice (Cuesta et al., 2012), and cannot be induced in ~95% of R6/2 mice, even at a presymptomatic age (2 months). Thus, MASCO output is disrupted several weeks before the locomotor circadian activity rhythms disintegrate (Cuesta et al., 2012). It is not clear what role the MASCO plays, if any, in humans. We suggest that whatever its role, since MASCO output is disrupted so early in R6/2 mice, this may contribute directly to the early symptoms of HD.

Since MASCO-dependent rhythms cannot be observed in R6/2 mice, they are unsuitable for detailed study of disruption of MASCO output. A number of 'knock-in' HD mouse models exist that have a slower progression of disease and more faithfully recapitulate the genetic context of HD mutation than does the R6/2 mouse (Menalled et al., 2009; Menalled, 2005). Here we used one such line to study MASCO ouput in HD, the Q175 mouse. Q175 mice are a full length knock-in model expressing a chimeric mouse/human exon 1 with a CAG repeat expansion of around 188 (Menalled et al., 2012). HOM Q175 mice exhibit robust behavioural and molecular abnormalities (Menalled et al., 2012). They show locomotor hypoactivity and rotarod deficit by ~7 months of age and a lifespan of ~2 years. These are preceded by a decrease in striatal gene markers from ~3 months of age. HET Q175 mice also exhibit behavioural deficits with a slower time course. Finally, it has recently been reported that Q175 mice have sleep and circadian deficits that recapitulate those seen in R6/2 mice and HD patients (Fisher et al., 2016; Loh et al., 2013), making the Q175 mouse line particularly suitable for studying MASCO-driven rhythms.

When we investigated circadian rhythms in Q175 mice, we found that both circadian rhythms driven by SCN and MASCO were disrupted in this line. As seen in R6/2 mice, induction

of the MASCO output in Q175 mice was impaired long before the disruption of SCN-mediated rest-activity rhythms was seen. Disruption of MASCO-driven rhythms in Q175 mice were progressive and gene dose-dependent. The disruption or absence of the MASCO-driven rhythms in old Q175 mice can be explained by three possibilities. First, they may not be expressed in old Q175 mice. Secondly, their disruption may be due to a decrease in sensitivity to methamphetamine, with the dose of 0.005% methamphetamine no longer sufficient to induce the MASCO-driven behaviour rhythm in Q175 mice. Finally, MASCO-driven rhythms may be expressed in old Q175 mice, but their period may be shortened as aging progressed. If this is the case, therefore, they may be masked by the suprachiasmatic nucleus-driven rhythm, as seen in C3H mice (Tataroglu et al., 2006).

Our findings support the idea that disruption of MASCO output may contribute to early behavioural changes in Q175 mice. The HD gene dose-dependence of impairments of MASCO output expression is a strong indicator that abnormalities in MASCO output may contribute to the circadian phenotype in HD.

2. Materials and methods

2.1. Animals

All experiments were conducted under the UK Animals (Scientific Procedures) Act 1986 with the approval of the University of Cambridge Animal Welfare and Ethical Review Body. WT and Q175 mice on a C57Bl6/J background were taken from a colony established in the University of Cambridge. The Cambridge colony originated from founders obtained from the Jackson Laboratory (Bar Harbor, Maine, USA). The Q175 line carried the HD mutation in an *HTT* exon 1

'knocked' into the mouse huntingtin gene. Age-matched HOM, HET and WT mice were generated by crossing HET Q175 mice on a C57Bl/6J background. Genotyping and determination of the CAG repeat length was carried out on tail biopsies by Laragen (Los Angeles, USA) using GeneMapper. All mice models of HD have longer CAG repeat lengths (between 110 and 300 in the most used R6/2 mice, and 175 in the mice we used in this study) compared to human HD (Menalled et al., 2009). In the first experiment, we characterised rest-activity rhythms of 2 groups of Q175 mice, one aged 3 months at the start of testing and one aged ~19 months. The group tested at 3 months of age was composed of: 14 WT (7 male and 7 female mice), 16 HET (11 male and 5 female mice) with a CAG repeat length of 180 ± 2 and 6 HOM mice (3 male and 3 female mice) with a CAG repeat length of 178 ± 1 for the shorter allele and 183 ± 2 for the longer allele. The group tested at 19 months of age was composed of 3 WT (2 male and 1 female mice), 8 HET (5 male and 3 female mice) with a CAG repeat length of 190 ± 4 and 4 HOM (3 male and 1 female) mice with a CAG repeat length of 180 ± 4 for the shorter allele and 192 ± 3 for the longer allele. Mice were tested for 4 weeks.

In a second experiment, we examined induction of MASCO output in a total of 74 mice (23 WT and 27 HET and 24 HOM mice), distributed into three experimental groups by age (Groups 1-3). Group 1 mice were treated with MAP from 2 months of age (9 to 17 weeks) for 8 weeks: 7 WT (4 male and 3 female mice), 11 HET (3 male and 8 female mice) with a CAG repeat length of 177 ± 3 and 6 HOM (2 male and 4 female mice) with a CAG repeat length of 162 ± 5 for the shorter allele and 172 ± 3 for the longer allele. Group 2 mice were treated from ~6 months (25 to 33 weeks) of age with MAP for 8 weeks: 7 WT (3 male and 4 female mice), 7 HET (4 male and 3 female mice) with a CAG repeat length of 176 ± 5 and 7 HOM (3 male and 4 female mice) with a CAG repeat length of 169 ± 7 for the shorter allele and 189 ± 7 for the longer allele. Group 3 mice

were treated from ~1 year of age (49 to 56 weeks) with MAP for 8 weeks: 9 WT (5 male and 4 female mice), 9 HET (4 male and 5 female mice) with a CAG repeat length of 175 ± 2 and 11 HOM (6 male and 5 female mice) with a CAG repeat length of 170 ± 2 for the shorter allele and 173 ± 3 for the longer allele.

In a third experiment, we repeated the exposure to MAP of mice from Group 1, Experiment 2. After a period without drug of 8 weeks, the mice from this group were re-exposed to MAP for 8 weeks at 6 months of age.

2.2. Husbandry

Mice were kept in weaning cages of up to 10 animals of same sex and mixed genotype per cage until the experiments started. Mice were kept in a controlled environment with 12:12 light-dark (LD) cycle, at a room temperature of 21°-23°C and humidity of 55% ± 10, with *ad libitum* access to dry laboratory food and water. Circadian studies were conducted with mice housed individually in a light-tight Scantainer ventilated cabinet (Scanbur, Denmark) with controlled humidity (55% ± 10) and temperature (21°-23°C).

For the first experiment, mice were placed in a 12:12 LD cycle for 7 days for habituation to the cabinet, then their circadian locomotor activity was monitored for 14 days in 12:12 LD cycle followed by 14 days in DD in order to assess the age where the circadian breakdown occurs in the Q175 knock-in model.

For the second and third experiments, mice were placed for ~7 days under a 12:12 LD cycle for habituation. The lights were then switched off and the mice remained in DD for the rest of the experiment.

2.3. Circadian analysis

We used passive infrared motion detectors (DS936, Bosch, Germany) placed on the top of each mouse cage to measure general patterns of activity continuously throughout the experiments for each individual mouse, and used Clocklab software (Actimetrics, Willmette, USA) to collect and analyse the circadian data. General activity was double plotted in actograms binned into 5-minute block size.

For the analysis of the circadian parameters, the first experiment was decomposed into 2 x 2 week periods comparing the 2 weeks in 12:12 LD cycle and the 2 weeks in DD. The second and third experiments were decomposed into 11 x 1 week periods that were: 1 week of pre-drug treatment (water), 8 weeks of MAP treatment and 2 weeks of drug withdrawal (water).

Mice were classified into two groups, according to whether or not they were expressing one or two components of activity. The first group was composed of mice that did not express MASCO-driven rhythms and showed only an SCN component. The second group was composed of mice that expressed both MASCO-driven rhythms and SCN component. The rest-activity patterns affected by the MAP treatment varied between mice within the same group, with the overall pattern depending on the competition between the behavioural rhythms generated by SCN and MASCO.

Period length was analysed using the actogram window in Clocklab. Activity onsets were manually determined for the 7 (Experiments 2-3) or 14 (Experiment 1) continuous days to be analysed. A least-square fits regression line was used to determine the corresponding period length. Duration of active period (alpha) of the SCN-driven rhythms was calculated as the difference

between the means of the regression lines drawn through the 7 or 14 activity onsets and corresponding offsets. For the occasional days where offsets of MASCO-driven rhythms were masking the offsets of SCN-driven rhythms, we omitted these days in the analysis. The distribution of the general activity during active and rest period was determined using the profile activity function of the software. Rest-activity ratio were calculated as the amount of activity occurring during the rest period as a fraction of the amount of total activity. In nocturnal animals, such as mice, it has been demonstrated that lower ratios reflect stronger rest-activity rhythms. Kaplan–Meier survival curves were used to compare the timing of the expression of the MASCO-driven rhythms (experiment 2-3). The Chi-squared periodograms (obtained with Clocklab) were used to determine behavioural rhythmicity in untreated mice. For mice treated with MAP, Lomb-Scargle periodograms were used as they are more appropriate due to the unequally spaced time data (Ruf, 1999) resulting from the complexity of the activity patterns caused by MAP treatment (Blum et al., 2014).

2.4. Methamphetamine treatment to induce MASCO-driven rhythms

Methamphetamine hydrochloride (M8750, Sigma Aldrich, UK) was administered to the mice via the drinking water at a low concentration (0.005% w/v) as previously described (Cuesta et al., 2012). Water bottles were weighed every 3 to 4 days to monitor drug consumption. Mice were weighed once weekly throughout the MAP treatment. We monitored dehydration by pinching the skin over the shoulder blades of the mice (Burkholder et al., 2012). During this study, we did not observe any cases of dehydration.

2.5. Statistics

Unless otherwise stated, all data are expressed as mean ± SEM. There was no significant sex difference found in any of the circadian parameters analysed, therefore, apart from data from body weight, all data from mice of both sex were pooled for presentation. Statistical analyses were performed using Statistica 19.0 software (version 12, StatSoft Inc., Tulsa, USA) or Prism 5 (GraphPad Software Inc., San Diego, USA). Analyse of variance (ANOVA) with repeated measures was performed to investigate differences between groups, followed by post hoc Student Newman Keuls test. Kaplan–Meier survival curves were analysed using Log-rank test. The results were considered significant when $P < 0.05$.

3. Results

3.1. Disintegration of circadian rhythms is late in Q175 mice

We first confirmed that there was an abnormal behavioural circadian phenotype in the Q175 mice. We characterised the locomotor circadian activity rhythm of WT, HET and HOM mice at two different ages in 12:12 LD cycle then in DD. Typical actograms and their corresponding periodograms are shown in Figures 1 and 2, at 3 and 19 months respectively. All Q175 mice tested at 3 months had robust rest-activity rhythms (Figs. 1A-I). At this age, there was no significant difference in the rest-activity ratio or period length between the three genotypes either in 12:12 LD (24 ± 0.01 h for WT, 23.99 ± 0.01 h for HET and 24.02 ± 0.01 h for HOM mice) or in DD (Figs. 3A and C).

By contrast to the 3 month old mice, in ‘elderly’ mice aged 19 months, significant differences were seen in both parameters (Figs. 3B, D). While all the HET mice were still rhythmic in both

LD and DD (Figs. 2B, E, H), half of the HOM mice showed signs of arrhythmicity (Figs. 2C, F, I; Fig. 3D). While the period length was similar in 12:12 LD cycle in all three genotypes (Fig. 3B), there was a disease-related effect on the free-running period length in DD [$F_{(2,13)} = 17$; $P < 0.001$], with the period length being shorter in HOM mice than it was in WT or HET mice ($P < 0.001$). There was a significant genotype effect [$F_{(2,13)} = 7.8$, $P < 0.01$] on the rest-activity ratio that was significantly increased in LD in elderly HOM mice compared to age-matched WT and HET mice ($P < 0.01$; Fig. 2D). There was no effect of genotype or age on the amplitude of the rhythms (Figs. 3E, F).

3.2. Expression of MASCO-driven rhythms is delayed or not induced in rhythmic Q175 mice

All Q175 mice up to 1 year of age that were tested with methamphetamine exhibited SCN-mediated circadian locomotor activity with a period length close to 24h, regardless of genotype (Figs. 4A-I). The only SCN deficits seen were in 2 out of 11 HOM mice that showed less robust rest-activity rhythm at the end of the experiment than expected, with a shortening of the free-running SCN period (see example actogram in Fig. 4I). Not all the mice developed a MASCO-dependent component in response to MAP (Figs. 4F, H, I). In WT mice a MASCO output was present in all mice at both 2 (Fig. 4A, J) and 6 months (Fig. 4D, J). By 1 year of age, however, a MASCO output such as that seen in Fig. 4G could be observed in only about half of the WT mice (Fig. 4J**)**. In HET mice, MASCO-driven rhythms were observed in all mice at 2 months (Figs. 4B, K), but in fewer than 50% of mice at 6 months (Fig. 4E, K), and only in 22% of mice when treated at 1 year (Figs. 4H, K). In HOM mice (Figs. 4C, F, I), MASCO component was observed in all mice at 2 months, but only in 14 and 9% of mice at 6 and 12 months respectively (Fig. 4L). Thus,

MASCO-driven rhythms are progressively disrupted in an HD gene dose-dependent manner. Notably, expression of MASCO-driven rhythms is also age-dependent.

3.3. Abnormalities in MASCO-driven rhythms are not due to decreased MAP consumption in Q175 mice

The inability to induce MASCO-driven rhythms in HET and HOM mice was not due to a decreased consumption of MAP by these mice. There was no difference between the amount of MAP drunk by any group at 2 (Fig. 5A) and 6 months (Fig. 5B). At 1 year of age, HOM mice actually consumed significantly more MAP compared to WT and HET mice (Fig. 5C). Interestingly, although they consumed more MAP, HOM mice still did not develop a MASCO component. At 2 and 6 months, the low dose of MAP treatment did not affect the weight gain due to growth of mice of any genotype (Figs. 6A, B, D, E), until 1 year of age, at which time male (but not female) HOM mice were significantly lighter than WT mice (Figs. 6C, F). This was expected due to disease-related changes (Fisher et al., 2016; Menalled et al., 2012).

3.4. Effect of age on expression of MASCO-driven rhythms

The timing of the MASCO component expression after commencement of MAP treatment was age-dependent, appearing sooner in young mice than it did in older mice (Figs. 7A-C). The time from beginning of treatment to appearance of MASCO-driven rhythms also depended on genotype. In presymptomatic mice (treated with MAP at 2 months of age), the MASCO component started to appear at around 1 week and was established within 4.5 weeks of the start of treatment, regardless of genotype (Fig. 7A). At 6 months of age, all WT mice developed the MASCO component between 2.5 and 4.5 weeks of treatment (Fig. 7B). By contrast, the MASCO output was observed either later in HET and HOM mice or did not appear at all within the 8 weeks of MAP treatment (Fig. 7B). A Log-rank test revealed a significant difference between start of MASCO-driven rhythms in WT and HET mice ($P < 0.01$) and between WT and HOM mice ($P < 0.001$). At 1 year of age, not all the WT mice expressed the MASCO-driven rhythms, with 40% of the WT mice developing it within the three first weeks of MAP treatment, 20% between 3 and 6.5 weeks (Fig. 7C) and the remaining 40% not developing a MASCO component within the 8 weeks of MAP treatment. Nevertheless, when a MASCO component developed in WT mice, it still appeared earlier than it did in HOM mice (Log-rank test, $P < 0.01$). The only HOM mouse (out of 11 tested) to develop a MASCO did so during week 7 of MAP treatment.

About a quarter of the WT mice treated with MAP expressed a MASCO component with a period length in the circabidian (48 hours) range (0/7 mice tested at 2, 3/7 mice tested at 6, and 3/9 mice tested at 12 months of age; Table 1 and Figs. 8A, D and G). It was notable that during the whole study, only 3 Q175 mice expressed circabidian rhythms (Table 1 and Figs. 8B, C and E). These were one HET and one HOM mice aged 2 months (Figs. 8B and C) and one HET mouse aged 6 months (Fig. 8E).

3.5. Effect of MAP on circadian parameters in Q175 mice

Among the other circadian parameters analysed, we confirmed that, as seen previously (Cuesta et al., 2012), MAP induced a significant lengthening of alpha across the 8 weeks of treatment for all mice in which testing started at 2 months (Supplementary Fig. 1). The lengthening of alpha caused by MAP declined with genotype and age (treatment effect, [$F_{(10,640)} = 99.49$; $P < 0.001$]; treatment x genotype interaction, [$F_{(20,640)} = 2.32$; $P < 0.001$]; treatment x age interaction, [$F_{(20,640)} = 4.68$; $P < 0.001$]). The effects of MAP on alpha, as with period length, were reversible, disappearing 2 to 3 days following MAP withdrawal (Supplementary Fig. 1).

Although MAP is a stimulant drug, the low doses used here did not have a major effect on locomotion. Total activity did not change with MAP at either 6 months or 1 year of age (Table 2). MAP significantly increased the total activity only in mice tested at 2 months (in WT mice for weeks 1, 3-5, in HET mice for weeks 2-8 and in HOM mice for week 2). The rest-activity ratio was not affected by MAP treatment in any of the groups at any time, regardless of age or genotype (data not shown).

3.6. Prior conditioning with methamphetamine delays the disruption of MASCO-driven rhythms in Q175 mice

In a third experiment, mice that had been given MAP previously at 2 months were treated a second time at 6 months of age. Typical actograms and corresponding periodograms are shown in Fig. 9. All WT mice expressed a MASCO component when treated a second time (Figs. 9D, G; Table 3). Interestingly, the appearance of MASCO-driven rhythms occurred significantly earlier in WT mice

that had been pre-exposed to MAP than was seen in naïve WT mice (Log rank test, $P < 0.01$; Fig. 9G). The second exposure to MAP also induced the expression of the MASCO-driven rhythms earlier in HET mice than was seen in the naïve group (Log-rank test, $P < 0.05$; Figs. 9B, E, H). Furthermore, whereas a MASCO output was observed in only 40% of naïve HET mice, 90% of HET mice pre-exposed to MAP subsequently expressed a MASCO output (Fig. 9H). Finally, whereas only 1 of the 7 naïve HOM mice treated at 6 months expressed MASCO-driven rhythms (Table 3, Fig. 9I), half of the HOM mice pre-exposed to MAP at the age of 2 months displayed a MASCO output at 6 months, although the rhythms in these HOM mice were very unstable (Table 3, Figs. 9F, I).

The second exposure to MAP had a main effect on the lengthening of alpha (MAP treatment x duration of MAP treatment, [$F_{(10,420)} = 2.15$, $P < 0.05$]; Supplementary Fig. 2), with an increase observed in pre-exposed compared to naïve WT (duration of MAP treatment: [$F_{(1,15)} = 18.75$; $P < 0.001$]; Supplementary Fig. 2A) and HOM mice [$F_{(1,11)} = 11.83$; $P < 0.01$] (Supplementary Fig. 2C). The second exposure to MAP had no effect on either total activity or rest-activity ratios (data not shown).

4. Discussion

Sleep and circadian disturbances are common symptoms of HD (Arnulf et al., 2008; Lazar et al., 2015; Morton, 2013; Morton et al., 2005; Piano et al., 2015). We showed previously that MASCO-driven rhythms were disrupted in the transgenic R6/2 fragment mouse model of HD (Cuesta et al., 2012). Here we show that this is also the case in the Q175 HD mouse. This is a line of mice that has a more relevant genetic context of the HD mutation than does the R6/2 mouse.

Our study provides the first evidence to our knowledge that the HD mutation affects circadian function in a gene dose-dependent manner, with the abnormalities in MASCO-driven rhythms of HOM Q175 mice being more pronounced and appearing earlier than they are in HET mice. It is already known that Q175 mice show a decline in circadian rhythms and sleep-wake cycle abnormalities (Fisher et al., 2016; Loh et al., 2013). Disruption of the MASCO-driven rhythms in Q175 mice appear before onset of other behavioural abnormalities, and many months before SCN circadian deficits appeared. We found a disruption in the expression of MASCO-driven rhythms from the age of 25 weeks in HET and HOM mice when they were still behaviourally normal. Others have shown that there are no locomotor deficits measurable until ~30-33 weeks, when rotarod and climbing deficits appeared in HOM mice (Menalled et al., 2012). Moreover, cognitive deficits are not present before 1 year and appear only in HOM mice (Menalled et al., 2012). However, morphological changes are almost certain to be already present at 25 weeks, since early eletrophysiological abnormalities have been reported beginning at 8 weeks (Indersmitten et al., 2015), and a decrease in spine density of medium-sized spiny neurons is present in HET and HOM mice at 7 and 12 months but not at 2 months. There was no correlation between the expression of the MASCO-driven rhythms and the robustness of the circadian locomotor activity. That is, the mice with disrupted MASCO-driven rhythms were not necessarily the ones with the more disrupted circadian locomotor activity rhythms. Furthermore, there were some mice in which MASCO could not be induced that had very robust circadian rhythms (see for example, actograms in Figs. 4F, 9C). The deficits in MASCO output we observe add to the repertoire of abnormal circadian behaviours in HD mice. Disruption of MASCO-driven rhythms are thus likely to be a pathological component relevant to HD.

The expression of the MASCO-driven rhythms was affected by age, not only in the Q175 mice, but also in WT mice. Indeed, MASCO output was disrupted in almost half of the 12 month-old WT mice treated with MAP. It has been shown by others that aging alters SCN-driven behavioural circadian rhythms such as locomotor activity, drinking behaviour, sleep-wake cycle and body temperature in WT rodents (Valentinuzzi et al., 1997; Van Gool and Mirmiran, 1983; Weinert and Waterhouse, 2007; Weinert, 2010, 2000; Witting et al., 1994; Yamazaki et al., 2002). Moreover, ageing is also accompanied by a decrease in the amplitude of the circadian locomotor rhythms (Valentinuzzi et al., 1997; Weinert et al., 2000; Yamasaki et al., 2002). This might also contribute to the disruption in the generation of the MASCO-driven rhythms. The age-dependent deficit of the MASCO-driven rhythm seen in Q175 mice could be the consequence of both aging and HD gene-related disease progression.

MASCO is an oscillator inducible by MAP. Since the primary action of MAP on dopaminergic neurons is to increase extracellular dopamine (DA), an intact dopaminergic system is likely to be crucial for the normal generation of the MASCO-driven rhythms. This is particularly relevant to HD, since aberrant dopaminergic transmission is thought to underlie many of the signs and symptoms of HD, especially the debilitating loss of control of movement and cognitive function (Bäckman and Farde, 2001; Chen et al., 2013; Guo et al., 2012; Squitieri et al., 2015; Tyebji et al., 2015), and psychiatric disturbances (Covey et al., 2016). There is considerable evidence for dysfunctional dopaminergic neurotransmission in HD patients and mouse models. In HD patients, DA signalling is disrupted, and both striatal DA (Bernheimer et al., 1973; Kish et al., 1987), and D1 and D2 receptor levels (Andrews et al., 1999; Antonini et al., 1996; Ginovart et al., 1997) are reduced. Post-mortem analyses of HD brain also show reduced transporter binding (Bäckman et al., 1997; Bernheimer et al., 1973; Ginovart et al., 1997; Glass et al., 2000; Kish et al., 1987; Suzuki

et al., 2001) and decreased levels of tyrosine hydroxylase that is the rate-limiting enzyme in DA synthesis (Yohrling et al., 2003). A number of studies have demonstrated a decrease in DA and DA receptors in HD mice (Callahan and Abercrombie, 2015; Cha et al., 1998; Hickey et al., 2002; Johnson et al., 2006; Mochel et al., 2011; Ortiz et al., 2010; Pouladi et al., 2012). Particularly relevant to this study is that altered DA function has been documented in 12-month old Q175 mice (Rothe et al., 2015; Smith et al., 2014). The fact that the disruption of the MASCO-dependent rhythms in R6/2 mice could be partially rescued by a treatment with L-DOPA (Cuesta et al., 2012) is also relevant to highlight the role of DA, since L-DOPA is the precursor for DA. Together, our data strongly support the idea that a defective dopaminergic neurotransmission prevents the expression of the MASCO-driven rhythms in R6/2 mice and by extension, Q175 mice, given that they exhibit similar circadian and sleep disturbances as R6/2 mice.

A study by Blum and colleagues has highlighted a possible mechanism for DA in the induction of MASCO-dependent rhythms that is consistent with the deficits we see in HD mice (Blum et al., 2014). These authors proposed that MAP-induced changes in DA ultradian oscillators explain the generation of MASCO-driven rhythms. DA levels fluctuate in the striatum with ultradian activity cycles. They showed that when chronic MAP increases the tone of the DA system, the period of the ultradian rhythms increases to infradian (>24 h) ranges, causing them to become desynchronised from the SCN rhythms and producing the aberrant patterns of locomotor activity that are manifested as MASCO output. By contrast, lowering the tone of the DA system shortened the period of the ultradian rhythms. We hypothesise that, dopamine system deficits in R6/2 and Q175 mice could contribute to the MASCO either being absent, or the MASCO-driven rhythms being disrupted, by either being shorter, harder to induce, or eventually not inducible at all.

It seems the neural networks that give rise to the MASCO-driven rhythms can be 'primed' so it is easier to induce their expression at an age when it would normally not be possible. Only one (out of 7) of the naïve HOM mice treated at 6 months developed a MASCO output, but after pre-treatment with MAP at 2 months, most HOM mice developed a MASCO output when MAP was given again at 6 months. At least one other study has shown a priming effect in the DA system (McFadden et al., 2015). In this study, rats that were self-administrating MAP for the first time had decreased striatal DAT and dopamine content, but this decrease was attenuated if the rats had prior MAP self-administration. A priming effect is also consistent with some of our pharmacological and behavioural studies where we showed that the neural circuitry in HD mice is not irreversibly damaged by the disease. For example, we have shown that drug treatment started presymptomatically can reverse dysregulation of clock genes expression and correct EEG abnormalities in R6/2 mice (Kantor et al., 2016; Pallier et al., 2007). In addition, circadian deficit in R6/2 mice can be delayed by bright light therapy started presymptomatically (Cuesta et al., 2014), and cognitive dysfunction can be improved by a therapeutic management of sleep-wake cycles (Pallier and Morton, 2009). Finally, we showed that L-DOPA chronic therapy improves motor deficits, although long term L-DOPA treatment had a deleterious effect on survival (Hickey et al., 2002). This latter study highlights the complexity of the role of dopaminergic neurotransmission in HD. Whereas an increase in DA level may be beneficial at presymptomatic or early stages, homeostatic decreases in DA may be protective at late symptomatic stages. Thus the pre-symptomatic stage seems to be the optimal time window for priming neural networks in HD brain to delay DA-mediated behavioural deficits. Translating this to HD patients, this emphasises the importance of understanding the optimal window of opportunity for particular therapies.

The role, indeed the very existence, of MASCO in humans is unknown. In mice, MASCO-driven rhythms expression requires isolation and treatment with chronic low dose of MAP for several weeks. It is not possible to reproduce the sort of studies performed in rodents to determine the existence of MASCO in humans. However, there is circumstantial evidence that a MASCO-like phenomenon might exist. MAP consumption disrupts circadian rhythms and sleep in humans (Hasler et al., 2012; Kirkpatrick et al., 2009). Moreover, studies of humans in isolation deprived of environmental cues revealed that the rest-activity rhythms can, and do, run at circadian periods greater than 24h (Aschoff and Wever, 1976; Mills et al., 1974; Wever, 1979). In one of these studies, one subject had a rest-activity rhythm period close to 33 hours, although the rhythm of their bodily functions remained close to 24 hours. Depriving humans of time cues seems to facilitate the emergence of an oscillator whose rhythms are desynchronised from the SCN. Another study, reporting the case of a healthy 20-year old student, showed that this desynchronization can also happen when a subject is not isolated from time cues (Wirz-Justice and Pringle, 1987). The subject in this study had no imperative time to wake up or go to sleep. He gradually developed long waking periods (up to the circabidian range) similar to the free-running period manifested by subjects isolated from time cues. His morning hormone measures, however, stayed within the normal range of SCN-driven circadian values. Although rare, these cases suggest in humans the existence of at least two independent endogenous oscillators underlying the temporal organisation of physiological processes. MASCO might be one of these oscillators, allowing rest-activity cycles to run with long periods when times cues are not present or not powerful enough to entrain the SCN. It seems equally possible that if the MASCO output is disrupted, it may contribute to a deleterious circadian phenotype. The clearest evidence for this comes from the HD mice with disrupted MASCO output (this study and Cuesta et al., 2012), and HD patients with abnormal

circadian behaviour (Morton, 2013; Morton et al., 2005). This may also be important in other diseases where the dopaminergic system is disrupted, such as Parkinson's disease (Bruguerolle and Simon, 2002; Mehta et al., 2008; Videnovic and Golombek, 2013), schizophrenia (Wulff et al., 2012), bipolar disorder (Berk et al., 2007; Harvey, 2008) and depression (Kronfeld-schor and Einat, 2012). These are all disorders in which alterations in rest-activity rhythms as well as motor and psychiatric disturbances have been reported (Jagannath et al., 2013; Videnovic et al., 2014; Wulff et al., 2010). In particular, aberrant sleep-wake timing with circabidian rhythms have been reported in schizophrenic (Wulff et al., 2009) and in manic-depressive patients (Wehr et al., 1983), resembling the specific rest-activity rhythms found in WT mice expressing MASCO-driven rhythms when chronically treated with MAP. Thus, in both psychiatric and neurodegenerative diseases, disruption of MASCO-driven rhythms could contribute to, or possibly even cause, the circadian abnormalities and resulting behavioural disturbances.

5. Conclusions

We have shown that the MASCO-driven rhythms are progressively impaired in the Q175 knock-in mouse model of HD, before any overt disruption of the SCN-mediated circadian locomotor activity. Mutant huntingtin affects MASCO output in a gene dose- and age-dependent manner, with the deficits appearing first in HOM mice, then in HET mice and finally in aged WT mice. By 1 year of age, ~90% of the Q175 HOM had disrupted MASCO-driven rhythms although they still showed circadian rhythmicity controlled by the SCN. We suggest that disruption of MASCO output is a marker of the defective dopaminergic neurotransmission in HD mice, and that this disruption could contribute to the circadian abnormalities and resulting behavioural disturbances in HD patients.

Funding

This work was supported by a grant from CHDI Foundation, *Inc*. (USA).

Acknowledgments

We thank Dr. Zhiguang Zheng and Mary Harding for technical assistance.

Conflict of interest statement

The authors declare that they have no conflict of interest.

REFERENCES

Andrews, T.C., Weeks, R.A., Turjanski, N., Gunn, R.N., Watkins, L.H., Sahakian, B., Hodges, J.R., Rosser, A.E., Wood, N.W., Brooks, D.J., 1999. Huntington's disease progression. PET and clinical observations. Brain 122, 2353–2363.

Antonini, A., Leenders, K.L., Spiegel, R., Meier, D., Vontobel, P., Weigell-Weber, M., Sanchez-Pernaute, R., de Yébenez, J.G., Boesiger, P., Weindl, A., Maguire, R.P., 1996. Striatal glucose metabolism and dopamine D2 receptor binding in asymptomatic gene carriers and patients with Huntington's disease. Brain 119, 2085–2095.

Arnulf, I., Nielsen, J., Lohmann, E., Schieffer, J., Wild, E., Jennum, P., Konofal, E., Walker, M., Oudiette, D., Tabrizi, S., Durr, A., 2008. Rapid eye movement sleep disturbances in Huntington Disease. Arch. Neurol. 65, 482–488.

Aschoff, J., Wever, R., 1976. Human circadian rhythms: a multioscillatory system. Fed. Proc. 35, 2326–2332.

Bäckman, L., Farde, L., 2001. Dopamine and cognitive functioning: Brain imaging findings in Huntington's disease and normal aging. Scand. J. Psychol. 42, 287–296.

Bäckman, L., Robins-Wahlin, T.B., Lundin, A., Ginovart, N., Farde, L., 1997. Cognitive deficits in Huntington's disease are predicted by dopaminergic PET markers and brain volumes. Brain 120, 2207–2217.

Bates, G.P., Dorsey, R., Gusella, J.F., Hayden, M.R., Kay, C., Leavitt, B.R., Nance, M., Ross, C.A., Scahill, R.I., Wetzel, R., Wild, E.J., Tabrizi, S.J., 2015. Huntington disease. Nat. Rev. Dis. Prim. 1, 15005.

Berk, M., Dodd, S., Kauer-Sant'Anna, M., Malhi, G., Bourin, M., Kapczinski, F., Norman, T., 2007. Dopamine dysregulation syndrome: implications for a dopamine hypothesis of bipolar disorder. Acta Psychiatr Scand 116, 41–49.

Bernheimer, H., Birkmayer, W., Hornykiewicz, O., Jellinger, K., Seitelberger, F., 1973. Brain dopamine and the syndromes of Parkinson and Huntington. Clinical, morphological and neurochemical correlations. J. Neurol. Sci. 20, 415–455.

Blum, I.D., Zhu, L., Moquin, L., Kokoeva, M. V, Gratton, A., Giros, B., Storch, K.-F., 2014. A highly tunable dopaminergic oscillator generates ultradian rhythms of behavioral arousal. Elife 3, e05105.

Bruguerolle, B., Simon, N., 2002. Biologic rhythms and Parkinson's disease: a chronopharmacologic approach to considering fluctuations in function. Clin. Neuropharmacol. 25, 194–201.

Burkholder, T., Foltz, C., Karlsson, E., Linton, C.G., Smith, J.M., 2012. Health evaluation of experimental laboratory mice. Curr. Protoc. Mouse Biol. 2, 145–165.

Callahan, J.W., Abercrombie, E.D., 2015. Relationship between subthalamic nucleus neuronal activity and electrocorticogram is altered in the R6/2 mouse model of Huntington's disease. J Physiol 16, 3727–3738.

Carter, R., Lione, L., Humby, T., Mangiarini, L., Mahal, A., Bates, G., Dunnett, S., Morton, A.J., 1999. Characterization of progressive motor deficits in mice transgenic for the human Huntington's disease mutation. J. Neurosci. 19, 3248–3257.

Cha, J.-H.J., Kosinski, C.M., Kerner, J.A., Alsdorf, S.A., Mangiarini, L., Davies, S.W., Penney, J.B., Bates, G.P., Young, A.B., 1998. Altered brain neurotransmitter receptors in transgenic mice expressing a portion of an abnormal human Huntington disease gene. PNAS 95, 6480–6485.

Chen, J.Y., Wang, E.A., Cepeda, C., Levine, M.S., 2013. Dopamine imbalance in Huntington's disease: a mechanism for the lack of behavioral flexibility. Front. Neurosci. 7, 114.

Covey, D.P., Dantrassy, H.M., Zlebnik, N.E., Gildish, I., Cheer, J.F., 2016. Compromised dopaminergic encoding of reward accompanying suppressed willingness to overcome high effort costs is a prominent prodromal characteristic of the Q175 mouse model of Huntington's disease. J. Neurosci. 36, 4993–5002.

Cuesta, M., Aungier, J., Morton, A.J., 2014. Behavioral therapy reverses circadian deficits in a transgenic mouse model of Huntington's disease. Neurobiol. Dis. 63, 85–91.

Cuesta, M., Aungier, J., Morton, A.J., 2012. The methamphetamine-sensitive circadian oscillator is dysfunctional in a transgenic mouse model of Huntington's disease. Neurobiol. Dis. 45, 145–155.

Fisher, S.P., Black, S.W., Schwartz, M.D., Wilk, A.J., Chen, T.-M., Lincoln, W.U., Liu, H.W., Kilduff, T.S., Morairty, S.R., 2013. Longitudinal analysis of the electroencephalogram and sleep phenotype in the R6/2 mouse model of Huntington's disease. Brain 136, 2159–2172.

Fisher, S.P., Schwartz, M.D., Wurts-Black, S., Thomas, A.M., Chen, T.-M., Miller, M.A., Palmerston, J.B., Kilduff, T.S., Morairty, S.R., 2016. Quantitative electroencephalographic analysis provides an early-stage indicator of disease onset and progression in the zQ175 knock-in mouse model of Huntington's disease. Sleep 39, 379–391.

Ginovart, N., Lundin, A., Farde, L., Halldin, C., Bäckman, L., Swahn, C.G., Pauli, S., Sedvall, G., 1997. PET study of the pre- and post-synaptic dopaminergic markers for the neurodegenerative process in Huntington's disease. Brain 120, 503–514.

Glass, M., Dragunow, M., Faull, R.L.M., 2000. The pattern of neurodegeneration in Huntington's disease: a comparative study of cannabinoid, dopamine, adenosine, and GABAA receptor alterations in the human basal ganglia in Huntington's disease. Neuroscience 97, 505–519.

Guo, Z., Rudow, G., Pletnikova, O., Codispoti, K., Orr, B.A., Crain, B.J., Duan, W., Margolis, R.L., Rosenblatt, A., Ross, C.A., Troncosco, J., 2012. Striatal neuronal loss correlates with clinical motor impairment in Huntington's disease. Mov. Disord. 27, 1379–1386.

Harvey, A.G., 2008. Sleep and circadian rhythms in bipolar disorder: seeking synchrony, harmony, and regulation. Am J Psychiatry 165, 820–829.

Hasler, B.P., Smith, L.J., Cousins, J.C., Bootzin, R.R., 2012. Circadian rhythms, sleep, and substance abuse. Sleep Med. Rev. 16, 67–81.

Hickey, M.A., Reynolds, G.P., Morton, A.J., 2002. The role of dopamine in motor symptoms in the R6/2 transgenic mouse model of Huntington's disease. J. Neurochem. 81, 46–59.

Honma, K., Honma, S., Hiroshige, T., 1987. Activity rhythms in the circadian domain appear in suprachiasmatic nuclei lesioned rats given methamphetamine. Physiol. Behav. 40, 767–774.

Honma, K., Honma, S., Hiroshige, T., 1986. Disorganization of the rat activity rhythm by chronic treatment with methamphetamine. Physiol. Behav. 38, 687–695.

Honma, S., Honma, K., Shirakawa, T., Hiroshige, T., 1988. Rhythms in behaviors, body temperature and plasma corticosterone in SCN lesioned rats given methamphetamine. Physiol. Behav. 44, 247–255.

Indersmitten, T., Tran, C.H., Cepeda, C., Levine, M.S., 2015. Altered excitatory and inhibitory inputs to striatal medium-sized spiny neurons and cortical pyramidal neurons in the Q175 mouse model of Huntington's disease. J. Neurophysiol. 113, 2953–2966.

Jagannath, A., Peirson, S.N., Foster, R.G., 2013. Sleep and circadian rhythm disruption in neuropsychiatric illness. Curr. Opin. Neurobiol. 23, 888–94.

Jeantet, Y., Cayzac, S., Cho, Y.H., 2013. β Oscillation during slow wave sleep and rapid eye movement sleep in the electroencephalogram of a transgenic mouse model of huntington's disease. PLoS One 8, e79509.

Johnson, M.A., Rajan, V., Miller, C.E., Wightman, R.M., 2006. Dopamine release is severely compromised in the R6/2 mouse model of Huntington's disease. J. Neurochem. 97, 737–746.

Kantor, S., Szabo, L., Varga, J., Cuesta, M., Morton, A.J., 2013. Progressive sleep and electroencephalogram changes in mice carrying the Huntington's disease mutation. Brain 136, 2147–2158.

Kantor, S., Varga, J., Morton, A.J., 2016. A single dose of hypnotic corrects sleep and EEG abnormalities in symptomatic Huntington's disease mice. Neuropharmacology 105, 298–307.

Kirkpatrick, M.G., Haney, M., Vosburg, S.K., Comer, S.D., Foltin, R.W., Hart, C.L., 2009.

Methamphetamine self-administration by humans subjected to abrupt shift and sleep schedule changes. Psychopharmacology (Berl). 203, 771–780.

Kish, S.J., Shannak, K., Hornykiewicz, O., 1987. Elevated serotonin and reduced dopamine in subregionally divided Huntington's disease striatum. Ann. Neurol. 22, 386–389.

Kronfeld-schor, N., Einat, H., 2012. Circadian rhythms and depression: Human psychopathology and animal models. Neuropharmacology 62, 101–114.

Kudo, T., Schroeder, A., Loh, D.H., Kuljis, D., Jordan, M.C., Roos, K.P., Colwell, C.S., 2011. Dysfunctions in circadian behavior and physiology in mouse models of Huntington's disease. Exp. Neurol. 228, 80–90.

Lazar, A.S., Panin, F., Goodman, A.O.G., Lazic, S.E., Lazar, Z.I., Mason, S.L., Rogers, L., Murgatroyd, P.R., Watson, L.P.E., Singh, P., Borowsky, B., Shneerson, J.M., Barker, R.A., 2015. Sleep deficits but no metabolic deficits in premanifest Huntington's disease. Ann. Neurol. 78, 630–648.

Lebreton, F., Cayzac, S., Pietropaolo, S., Jeantet, Y., Cho, Y.H., 2015. Sleep physiology alterations precede plethoric phenotypic changes in R6/1 Huntington's disease mice. PLoS One 10, 1–17.

Loh, D.H., Kudo, T., Truong, D., Wu, Y., Colwell, C.S., 2013. The Q175 mouse model of Huntington's disease shows gene dosage- and age-related decline in circadian rhythms of activity and sleep. PLoS One 8, e69993.

Mangiarini, L., Sathasivam, K., Seller, M., Cozens, B., Harper, A., Hetherington, C., Lawton, M., Trottier, Y., Lehrach, H., Davies, S.W., Bates, G.P., 1996. Exon 1 of the HD gene with an expanded CAG repeat is sufficient to cause a progressive neurological phenotype in transgenic mice. Cell 87, 493–506.

McFadden, L.M., Vieira-Brock, P.L., Hanson, G.R., Fleckenstein, A.E., 2015. Prior methamphetamine self-administration attenuates the dopaminergic deficits caused by a subsequent methamphetamine exposure. Neuropharmacology 93, 146–154.

Mehta, S.H., Morgan, J.C., Sethi, K.D., 2008. Sleep disorders associated with Parkinson's disease: role of dopamine, epidemiology, and clinical scales of assessment. CNS Spectr. 13, 6–11.

Menalled, L., El-Khodor, B.F., Patry, M., Suárez-Fariñas, M., Orenstein, S.J., Zahasky, B., Leahy, C., Wheeler, V., Yang, X.W., MacDonald, M., Morton, A.J., Bates, G., Leeds, J., Park, L., Howland, D., Signer, E., Tobin, A., Brunner, D., 2009. Systematic behavioral evaluation of Huntington's disease transgenic and knock-in mouse models. Neurobiol. Dis. 35, 319–336.

Menalled, L.B., 2005. Knock-in mouse models of Huntington's disease. NeuroRx 2, 465–470.

Menalled, L.B., Kudwa, A.E., Miller, S., Fitzpatrick, J., Watson-Johnson, J., Keating, N., Ruiz, M., Mushlin, R., Alosio, W., McConnell, K., Connor, D., Murphy, C., Oakeshott, S., Kwan, M., Beltran, J., Ghavami, A., Brunner, D., Park, L.C., Ramboz, S., Howland, D., 2012. Comprehensive behavioral and molecular characterization of a new knock-in mouse model of Huntington's disease: zQ175. PLoS One 7, e49838.

Mills, J.N., Minors, D.S., Waterhouse, J., 1974. The circadian rhythms of human subjects without

timepieces or indication of the alternation of day and night. J. Physiol. 240, 567–594.

Mochel, F., Durant, B., Durr, A., Schiffmann, R., 2011. Altered dopamine and serotonin metabolism in motorically asymptomatic R6/2 mice. PLoS One 6, e18336.

Morton, A.J., 2013. Circadian and sleep disorder in Huntington's disease. Exp. Neurol. 243, 34–44.

Morton, A.J., Wood, N.I., Hastings, M.H., Hurelbrink, C., Barker, R.A., Maywood, E.S., 2005. Disintegration of the sleep-wake cycle and circadian timing in Huntington's disease. J. Neurosci. 25, 157–163.

Ortiz, A.N., Kurth, B.J., Osterhaus, G.L., Johnson, M.A., 2010. Dysregulation of intracellular dopamine stores revealed in the R6/2 mouse striatum. J. Neurochem. 112, 755–761.

Pallier, P.N., Maywood, E.S., Zheng, Z., Chesham, J.E., Inyushkin, A.N., Dyball, R., Hastings, M.H., Morton, A.J., 2007. Pharmacological imposition of sleep slows cognitive decline and reverses dysregulation of circadian gene expression in a transgenic mouse model of Huntington's disease. Neurobiol. Dis. 27, 7869–7878.

Pallier, P.N., Morton, A.J., 2009. Management of sleep/wake cycles improves cognitive function in a transgenic mouse model of Huntington's disease. Brain Res. 1279, 90–98.

Piano, C., Losurdo, A., Della Marca, G., Solito, M., Calandra-Buonaura, G., Provini, F., Bentivoglio, A.R., Cortelli, P., 2015. Polysomnographic findings and clinical correlates in Huntington Disease: a cross-sectional cohort study. Sleep 38, 1489–1495.

Pouladi, M.A., Stanek, L.M., Xie, Y., Franciosi, S., Southwell, A.L., Deng, Y., Butland, S., Zhang, W., Cheng, S.H., Shihabuddin, L.S., Hayden, M.R., 2012. Marked differences in neurochemistry and aggregates despite similar behavioural and neuropathological features of Huntington disease in the full-length BACHD and YAC128 mice. Hum. Mol. Genet. 21, 2219–2232.

Rothe, T., Deliano, M., Wójtowicz, A.M., Dvorzhak, A., Harnack, D., Paul, S., Vagner, T., Melnick, I., Stark, H., Grantyn, R., 2015. Pathological gamma oscillations, impaired dopamine release, synapse loss and reduced dynamic range of unitary glutamatergic synaptic transmission in the striatum of hypokinetic Q175 Huntington mice. Neuroscience 311, 519–538.

Ruf, T., 1999. The Lomb-Scargle periodogram in biological rhythm research: analysis of imcomplete and unequally spaced time-series. Biol. Rhythm Res. 30, 178–201.

Smith, G.A., Rocha, E.M., McLean, J.R., Hayes, M.A., Izen, S.C., Isacson, O., Hallett, P.J., 2014. Progressive axonal transport and synaptic protein changes correlate with behavioral and neuropathological abnormalities in the heterozygous Q175 KI mouse model of Huntington's disease. Hum. Mol. Genet. 23, 4510–4527.

Squitieri, F., Di Pardo, A., Favellato, M., Amico, E., Maglione, V., Frati, L., 2015. Pridopidine, a dopamine stabilizer, improves motor performance and shows neuroprotective effects in Huntington disease R6/2 mouse model. J. Cell. Mol. Med. 19, 2540–2548.

Squitieri, F., Gellera, C., Cannella, M., Mariotti, C., Cislaghi, G., Rubinsztein, D.C., Almqvist,

E.W., Turner, D., Bachoud-Lévi, A.-C., Simpson, S.A., Delatycki, M., Maglione, V., Hayden, M.R., Donato, S. Di, 2003. Homozygosity for CAG mutation in Huntington disease is associated with a more severe clinical course. Brain 126, 946–955.

Suzuki, M., Desmond, T.J., Albin, R.L., Frey, K.A., 2001. Vesicular neurotransmitter transporters in Huntington's disease: initial observations and comparison with traditional synaptic markers. Synapse 41, 329–336.

Tataroglu, O., Davidson, A.J., Benvenuto, L.J., Menaker, M., 2006. The Methamphetamine-Sensitive Circadian Oscillator (MASCO) in Mice. J. Biol. Rhythms 21, 185–194.

The Huntington's Disease Collaborative Research group, 1993. A novel gene containing a trinucleotide that is expanded and unstable on Huntington's disease chromosomes. Cell 72, 971–983.

Tyebji, S., Saavedra, A., Canas, P.M., Pliassova, A., Delgado-García, J.M., Alberch, J., Cunha, R.A., Gruart, A., Pérez-Navarro, E., 2015. Hyperactivation of D1 and A2A receptors contributes to cognitive dysfunction in Huntington's disease. Neurobiol. Dis. 74, 41–57.

Valentinuzzi, V.S., Scarbrough, K., Takahashi, J.S., Turek, F.W., 1997. Effects of aging on the circadian rhythm of wheel-running activity in C57BL/6 mice. Am. J. Physiol. 273, R1957–1964.

Van Gool, W.A., Mirmiran, M., 1983. Age-related changes in the sleep pattern of male adult rats. Brain Res. 279, 394–398.

Videnovic, A., Golombek, D., 2013. Circadian and sleep disorders in Parkinson's disease. Exp. Neurol. 243, 45–56.

Videnovic, A., Lazar, A.S., Barker, R.A., Overeem, S., 2014. "The clocks that time us"—circadian rhythms in neurodegenerative disorders. Nat. Rev. Neurol. 10, 683–693.

Wehr, T.A., Sack, D., Rosenthal, N., Duncan, W., Gillin, J.C., 1983. Circadian rhythm disturbances in manic-depressive illness. Fed. Proc. 42, 2809–2814.

Weinert, D., 2010. Circadian temperature variation and ageing. Ageing Res. Rev. 9, 51–60.

Weinert, D., 2000. Age-dependent changes of the circadian system. Chronobiol. Int. 17, 261–283.

Weinert, D., Waterhouse, J., 2007. The circadian rhythm of core temperature: Effects of physical activity and aging. Physiol. Behav. 90, 246–256.

Wever, R.A., 1979. Influence of physical workload on freerunning circadian rhythms of man. Plügers Arch. 126, 119–126.

Wirz-Justice, A., Pringle, C., 1987. The non-entrained life of a young gentleman at Oxford. Sleep 10, 57–61.

Witting, W., Mirmiran, M., Bos, N.P., Swaab, D.F., 1994. The effect of old age on the free-running period of circadian rhythms in rat. Chronobiol. Int. 11, 103–112.

Wood, N.I., McAllister, C.J., Cuesta, M., Aungier, J., Fraenkel, E., Morton, A.J., 2013. Adaptation to experimental jet-lag in R6/2 mice despite circadian dysrhythmia. PLoS One 8, e55036.

Wulff, K., Dijk, D., Middleton, B., Foster, R.G., Joyce, E.M., 2012. Sleep and circadian rhythm disruption in schizophrenia. BJPsych 200, 308–316.

Wulff, K., Gatti, S., Wettstein, J.G., Foster, R.G., 2010. Sleep and circadian rhythm disruption in psychiatric and neurodegenerative disease. Nat. Rev. Neurosci. 11, 589–599.

Wulff, K., Porcheret, K., Cussans, E., Foster, R.G., 2009. Sleep and circadian rhythm disturbances: multiple genes and multiple phenotypes. Curr. Opin. Genet. Dev. 19, 237–246.

Yamazaki, S., Straume, M., Tei, H., Sakaki, Y., Menaker, M., Block, G.D., 2002. Effects of aging on central and peripheral mammalian clocks. PNAS. 99, 10801–10806.

Yohrling, G.J., Jiang, G.C., DeJohn, M.M., Miller, D.W., Young, A.B., Vrana, K.E., Cha, J.J., 2003. Analysis of cellular , transgenic and human models of Huntington's disease reveals tyrosine hydroxylase alterations and substantia nigra neuropathology. Mol. Brain Res. 119, 28–36.

Legends to figures.

Figure 1. Normal rest-activity patterns in young Q175 mice. Representative double-plotted actograms of wild-type (WT, A), heterozygous (HET, B) and homozygous (HOM, C) mice are shown from ~3 months (12 to 16 weeks) of age. Mice were placed in 12:12 light-dark (LD) for two weeks, followed by two weeks of constant darkness (DD). Chi-square periodograms are shown for LD (D- F) and DD (G- I) for WT (D, G), HET (E, H) and HOM (F, I) mice.

Figure 2. Circadian rhythm disruption in old homozygous Q175 mice. Representative double-plotted actograms of wild-type (WT, A), heterozygous (HET, B) and homozygous (HOM, C) mice are shown from ~19 months (82 to 86 weeks) of age. Mice were placed in 12:12 light-dark (LD) for two weeks, followed by two weeks of constant darkness (DD). Chi-square periodograms are shown for LD (D- F) and DD (G- I) for WT (D, G), HET (E, H) and HOM (F, I) mice.

Figure 3. Period length and rest-activity ratio become progressively abnormal in Q175 mice. Graphs show period length (A, B), rest-activity ratio (C, D) and amplitude of rhythms (E, F) in 12:12 light-dark (LD) and constant darkness (DD) for WT (black columns), HET (dashed columns) and HOM (white columns) mice at 3 months (A, C, E) and at 19 months of age (B, D, F). $^{**}P < 0.01$, $^{***}P < 0.001$. Statistical differences between LD and DD are not shown.

Figure 4. Expression of MASCO output declines in a gene dose- and age-dependent manner in Q175 mice. Representative double-plotted actograms (A-I, top panels) show general activity of

WT (A, D, G), HET (B, E, H) and HOM (C, F, I) mice placed in constant darkness and treated with 0.005% MAP for 8 weeks. Naïve mice were treated from 2 months (A- C), 6 months (D- F), or 12 months (G-I) of age. Note that other examples of naïve mice treated at 6 months are shown in Figure 9A-C. The asterisks indicate the start of the 8-week 0.005% MAP treatment. Lomb-Scargle periodograms (A-I, bottom panels) are shown for each actogram for the time window indicated by the black bars at the right of the actograms. The black dashed and red dotted lines on the actogram (A) represent the period length of SCN- and MASCO-driven rhythms, respectively. Histograms show the percentage of WT (J), HET (K) and HOM (L) mice expressing MASCO-driven rhythms within 8 weeks, where treatment starts at 2 (black columns), 6 (dashed columns) or 12 (white columns) months. Numbers of mice (out of the total number of mice tested) expressing MASCO-driven rhythms are indicated above each column.

Figure 5. Disruption of MASCO output in Q175 mice are not due to decreased MAP consumption. Graphs show average water consumption in ml/day/gram body weight for WT (black symbols), HET (grey symbols) and HOM (white symbols) mice treated with MAP from 2 (A), 6 (B) and 12 (C) months of age for 8 weeks followed by two weeks of drug withdrawal. In all panels, the bar above the x-axis indicates treatment with MAP (black bar) or water only (open bar). The asterisks and hashes indicate statistical comparison of HOM with WT mice and HOM with HET mice, respectively. No statistical difference was found between WT and HET mice. *$P < 0.05$, #$P < 0.05$.

Figure 6. Minor changes in body weight of mice during MAP treatment. Body weight was measured in WT (black symbols), HET (grey symbols) and HOM (white symbols) female (A-C) or male (D-F) mice at 2 (A, D), 6 (B, E) or 12 (C, F) months of age. In all panels, the bar above the x-axis indicates treatment with MAP (black) or water (open). Comparison of bodyweight of HOM with WT mice is indicated by asterisks. Where error bars are not visible, they are obscured by the symbols. *P < 0.05, **P < 0.01, ***P < 0.001.

Figure 7. Delays in timing of MASCO output expression are age- and gene dose-dependent in Q175 mice. Kaplan-Meier curves show cumulative percentage of mice that developed MASCO-driven rhythms during the 8 weeks of MAP treatment for WT (black symbols), HET (grey symbols) and HOM (white symbols) mice treated with MAP from 2 (A), 6 (B) or 12 (C) months of age. **P < 0.01, ***P < 0.001.

Figure 8. MAP-induced changes in rest-activity rhythms are gene dose-dependent in Q175 mice. Scatter plots (A-I) show period lengths of the rhythms driven by MASCO (white squares) or SCN (black squares) for each individual mouse during the experiment for WT (A, D, G), HET (B, E, H) and HOM (C, F, I) mice at 2 (A-C), 6 (D-F) or 12 (G-I) months of age. The bar above the x-axis indicates the treatment with MAP (black) or water (open).

Figure 9. Pre-conditioning with chronic MAP changes both onset and inducibility of MASCO output in Q175 mice. Representative double-plotted actograms (A-F, top panels) are shown from 6 months old WT (A, D), HET (B, E) and HOM (C, F) mice that were either naïve to

treatment (A-C) or pre-exposed to MAP (D-F) before start of treatment. The asterisks indicate the start of the 8-week 0.005% MAP treatment. Lomb-Scargle periodograms (A-I, bottom panels) are shown for each actogram for the time window indicated by the black bars at the right of the actograms. Graphs in G-I show the cumulative percentage of mice in which MASCO-driven rhythms were observed for each week of the experiment for WT (G), HET (H) and HOM (I) mice when naïve (black symbols) or pre-exposed to MAP (white symbols). *$P < 0.05$, **$P < 0.01$.

ABBREVIATIONS

ANOVA – analysis of variance

DA - dopamine

DD – constant darkness

HD – Huntington's disease

HET – heterozygous

HOM – homozygous

HTT – human Huntingtin gene

LD – 12:12 light-dark

MAP – methamphetamine

MASCO – methamphetamine-sensitive circadian oscillator

SCN – suprachiasmatic nucleus

WT– wild-type

Table 1. Effect of 0.005% methamphetamine on the period length of the MASCO-driven rhythms in WT, Q175 HET and Q175 HOM mice treated at 2, 6 or 12 months.

Treatment period	Genotype	Mean Period length(h) ± SEM (number of mice)					
		MASCO-driven rhythms (non circabidian)			MASCO-driven rhythms (circabidian)		
		2 months	6 months	12 months	2 months	6 months	12 months
week 1	WT	24.3 ± 0.1 (7)	ND	ND	ND	ND	ND
	HET	26.0 (1)	ND	ND	ND	ND	ND
	HOM	ND	ND	ND	ND	ND	ND
week 2	WT	26.3 ± 0.9 (6)	25.7 (1)	25.7 (1)	ND	ND	ND
	HET	25.7 ± 0.6 (4)	ND	ND	ND	ND	ND
	HOM	25.7 ± 0.6 (4)	ND	ND	ND	ND	ND
week 3	WT	26.6 ± 1.1 (7)	26.6 ± 1.4 (2)	26.0 ± 1.7 (3)	ND	ND	ND
	HET	26.2 ± 0.5 (8)	ND	ND	ND	ND	ND
	HOM	26.5 ± 1 (5)	ND	ND	ND	ND	ND
week 4	WT	26.6 ± 0.9 (7)	25.9 ± 0.7 (4)	26.1 ± 0.7 (3)	ND	48.7 (1)	ND
	HET	26.8 ± 0.5 (10)	ND	ND	ND	ND	ND
	HOM	26.0 ± 0.2 (5)	ND	ND	44.4 (1)	ND	ND
week 5	WT	26.5 ± 0.8 (7)	26.6 ± 0.7 (3)	26.8 (1)	ND	47.9 ± 0.6 (2)	48.0 (1)
	HET	27.3 ± 0.6 (10)	30.0 ± 3.7 (2)	ND	ND	ND	ND
	HOM	25.9 ± 0.3 (5)	ND	ND	46.6 (1)	ND	ND
week 6	WT	26.5 ± 0.7 (6)	26.9 ± 0.4 (4)	27.7 ± 1.9 (3)	ND	47.8 ± 0.6 (2)	48.0 (1)
	HET	26.1 ± 0.5 (11)	27.3 ± 0.3 (2)	26.5 (1)	ND	ND	ND
	HOM	25.3 ± 0.3 (5)	27.5 (1)	ND	48.2 (1)	ND	ND
week 7	WT	26.9 ± 0.79 (7)	29.4 ± 0.8 (5)	29.1 ± 1.6 (2)	ND	48.4 ± 0.3 (2)	47.7 ± 0.5 (2)
	HET	26.3 ± 0.6 (11)	26.4 ± 0.2 (2)	26.2 ± 0.8 (3)	ND	ND	ND
	HOM	26.9 ± 0.6 (5)	ND	ND	48.8 (1)	ND	ND
week 8	WT	27.8 ± 0.9 (7)	28.9 ± 1.3 (4)	26.5 ± 3.0 (2)	ND	47.4 ± 0.2 (3)	47.5 ± 0.6 (3)
	HET	28.3 ± 2.1 (10)	26.8 (1)	26.8 ± 0.3 (2)	48.4 (1)	47.5 (1)	ND
	HOM	26.4 ± 0.5 (5)	26.7 (1)	27.5 (1)	48.0 (1)	ND	ND

*P < 0.05, **P < 0.01, ***P < 0.001.

ND indicates that MASCO-driven rhythms are not detected in the corresponding group of mice

Table 2. Effect of chronic low dose of methamphetamine on the general activity in WT, Q175 HET and Q175 HOM mice

Treatment period	Genotype	Treatment	Mean Total activity counts/24 hours ± SEM (number of mice)		
			2 months	6 months	12 months
Pre-treatment	WT	Water alone	3659 ± 287 (7)	3279 ± 509 (7)	2163 ± 364 (9)
	HET		3579 ± 323 (11)	2304 ± 282 (7)	1683 ± 234 (9)
	HOM		2528 ± 338 (6)	1910 ± 405 (7)	2079 ± 292 (11)
MAP week 1	WT	MAP	5000 ± 327 (7)*	2797 ± 393 (7)	3576 ± 372 (9)
	HET		4640 ± 336 (11)	2358 ± 180 (7)	2524 ± 209 (9)
	HOM		3353 ± 540 (6)	2655 ± 460 (7)	2541 ± 351 (11)
MAP week 2	WT	MAP	4667 ± 364 (7)	2420 ± 534. (7)	2708 ± 520 (9)
	HET		4868 ± 242 (11)*	1946 ± 250 (7)	2624 ± 351 (9)
	HOM		3963 ± 431 (6)*	2759 ± 479 (7)	2304 ± 370 (7)
MAP week 3	WT	MAP	5117 ± 506 (7)*	3940 ± 382 (7)	2936 ± 485 (9)
	HET		5049 ± 303 (11)**	2615 ± 419 (7)	3166 ± 595 (9)
	HOM		3870 ± 201 (6)	2917 ± 578 (7)	2435 ± 278 (11)
MAP week 4	WT	MAP	5051 ± 399 (7)*	3129 ± 490 (7)	3324 ± 359 (9)
	HET		5332 ± 375 (11)***	2507 ± 236 (7)	2760 ± 595 (9)
	HOM		3506 ± 400 (6)	2271 ± 527 (7)	2292 ± 322 (11)
MAP week 5	WT	MAP	4861 ± 356 (7)***	3368 ± 464 (7)	3290 ± 298 (9)
	HET		4790 ± 362 (11)*	2540± 200 (7)	3028 ± 545 (9)
	HOM		3496 ± 296 (6)	2577 ± 636 (7)	2216 ± 287 (11)
MAP week 6	WT	MAP	5312 ± 490 (7)	3012 ± 165 (7)	3826 ± 267 (9)
	HET		5430 ± 368 (11)***	2600 ± 264 (7)	3028 ± 477 (9)
	HOM		3621 ± 470 (6)	2988 ± 734 (7)	2215 ± 264 (11)
MAP week 7	WT	MAP	4533 ± 391 (7)	3850 ± 376 (7)	3634 ± 283 (9)
	HET		4997 ± 412 (11)*	2757 ± 240 (7)	3102 ± 468 (9)
	HOM		3211 ± 380 (6)	2754 ± 598 (7)	2241 ± 329 (11)
MAP week 8	WT	MAP	4861 ± 593 (7)	3964 ± 441 (7)	3619 ± 290 (9)
	HET		4968 ± 370 (11)*	2626 ± 301 (7)	3241 ± 513 (9)
	HOM		3131 ± 349 (6)	2811 ± 602 (7)	2201 ± 355 (11)
withdrawal 1	WT	Water alone	2246 ± 282 (7)	2778 ± 327 (7)	2312 ± 277 (9)
	HET		3149 ± 438 (11)	2003 ± 219 (7)	1970 ± 169 (9)
	HOM		2145 ± 211 (6)	2182 ± 240. (7)	1924 ± 251 (11)
withdrawal 2	WT	Water alone	2237 ± 320 (7)	3061 ± 359 (7)	2305 ± 263 (9)
	HET		2978 ± 408 (11)	2013 ± 136 (7)	2167 ± 175 (9)
	HOM		2045 ± 221 (6)	2202 ± 345 (7)	1986 ± 270 (7)

*P < 0.05, **P < 0.01, ***P < 0.001 compared to pre-treatment week

Table 3. Effect of 0.005% methamphetamine on the period length of the MASCO-driven rhythms in naïve and drug pre-exposed WT, Q175 HET and Q175 HOM mice at the age of 6 months

Treatment period	Genotype	Number of mice with MASCO output/total		Mean Period length(h) ± SEM (number of mice)			
				MASCO-driven rhythms (non circadian)		MASCO-driven rhythms (circadian)	
		naïve	pre-exposed	naïve	pre-exposed	naïve	pre-exposed
week 1	WT	0/7	1/7	ND	24.7 (1)	ND	ND
	HET	0/7	1/11	ND	24.3 (1)	ND	ND
	HOM	0/7	0/6	ND	ND	ND	ND
week 2	WT	1/7	5/7	25.7 (1)	26.3 ± 0.7 (5)	ND	ND
	HET	0/7	3/11	ND	25.5 ± 0.8 (3)	ND	ND
	HOM	0/7	1/6	ND	25.3 (1)	ND	ND
week 3	WT	2/7	5/7	26.6 ± 1.4 (2)	26.7 ± 0.8 (5)	ND	ND
	HET	0/7	7/11	ND	25.9 ± 0.4 (7)	ND	ND
	HOM	0/7	1/6	ND	24.3 (1)	ND	ND
week 4	WT	5/7	6/7	25.9 ± 0.7 (4)	26.2 ± 0.8 (5)	48.8 (1)	53.1 (1)
	HET	0/7	7/11	ND	25.5 ± 0.4 (7)	ND	ND
	HOM	0/7	3/6	ND	26.5 ± 2.0 (3)	ND	ND
week 5	WT	5/7	7/7	26.6 ± 0.7 (3)	28.5 ± 1.2 (6)	47.9 ± 0.6 (2)	50.7 (1)
	HET	2/7	7/11	30.0 ± 3.7 (2)	27.1 ± 0.9 (7)	ND	ND
	HOM	0/7	2/6	ND	35.8 ± 13.0 (2)	ND	ND
week 6	WT	6/7	6/7	26.9 ± 0.4 (4)	28.2 ± 1.1 (6)	47.8 ± 0.6 (2)	ND
	HET	2/7	5/11	27.3 ± 0.3 (2)	25.2 ± 1.0 (3)	ND	46.1 ± 2.7 (2)
	HOM	1/7	1/6	27.5 (1)	25.8 (1)	ND	ND
week 7	WT	7/7	6/7	29.4 ± 0.8 (5)	30.5 ± 4.3 (5)	48.4 ± 0.3 (2)	49.9 (1)
	HET	2/7	9/11	26.4 ± 0.2 (2)	27.0 ± 1.2 (8)	ND	44.3 (1)
	HOM	0/7	1/6	ND	ND	ND	48.6 (1)
week 8	WT	7/7	6/7	28.9 ± 1.3 (4)	26.9 ± 1.2 (4)	47.4 ± 0.2 (3)	54.5 ±10.1 (2)
	HET	2/7	10/11	26.8 (1)	27.3 ± 1.4 (9)	47.5 (1)	48.5 (1)
	HOM	1/7	3/6	26.7 (1)	27.4 (1)	ND	49.0 ± 1.3 (2)

*P < 0.05, **P < 0.01, ***P < 0.001

ND indicates that MASCO-driven rhythms are not detected in the corresponding group

Figure 1

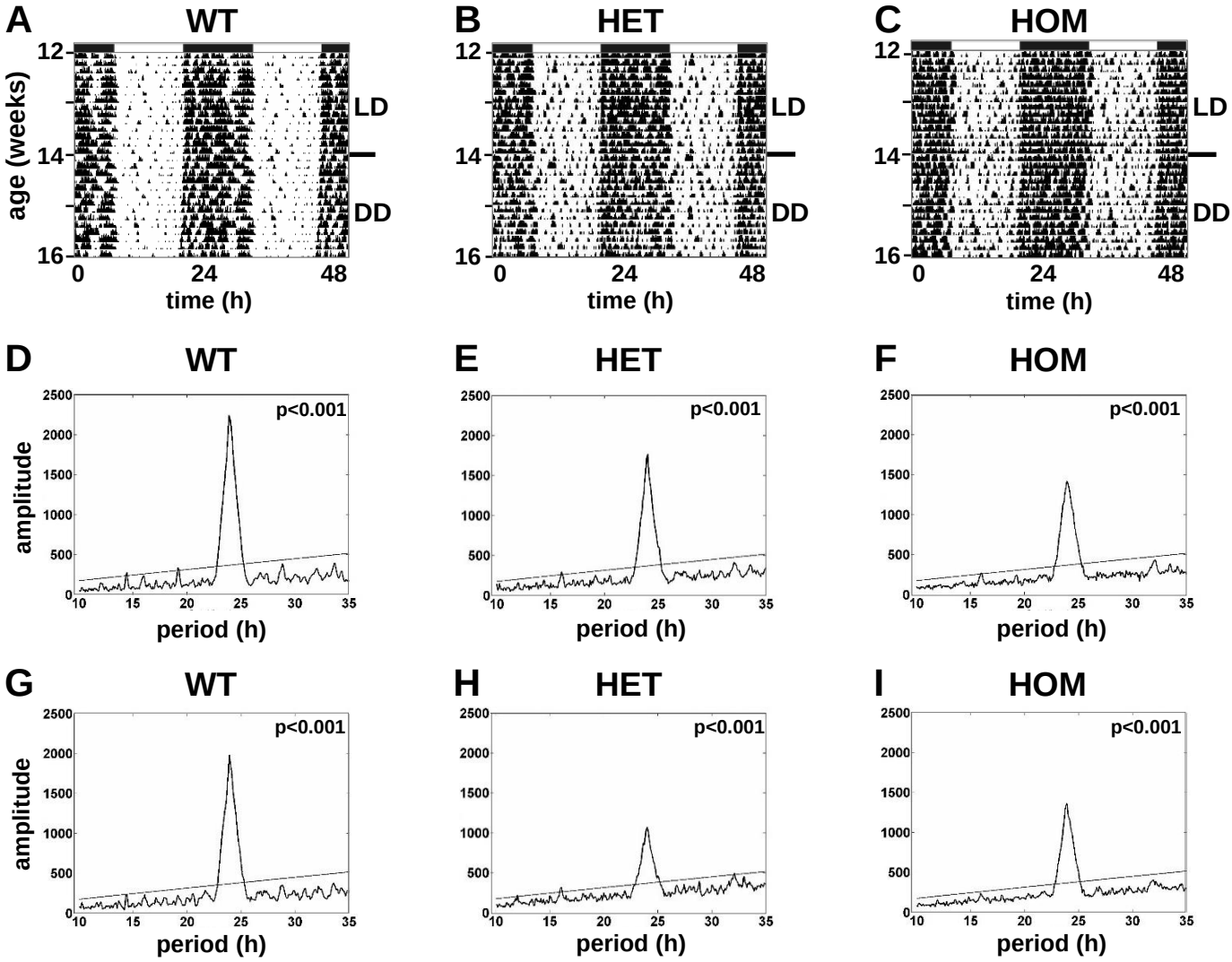
A
WT
B
HET
C
HOM
age (weeks)
12
14
16
LD
DD
0
24
48
time (h)
D
WT
E
HET
F
HOM
amplitude
p<0.001
2500
2000
1500
1000
500
0
10
15
20
25
30
35
period (h)
G
WT
H
HET
I
HOM

Figure 2

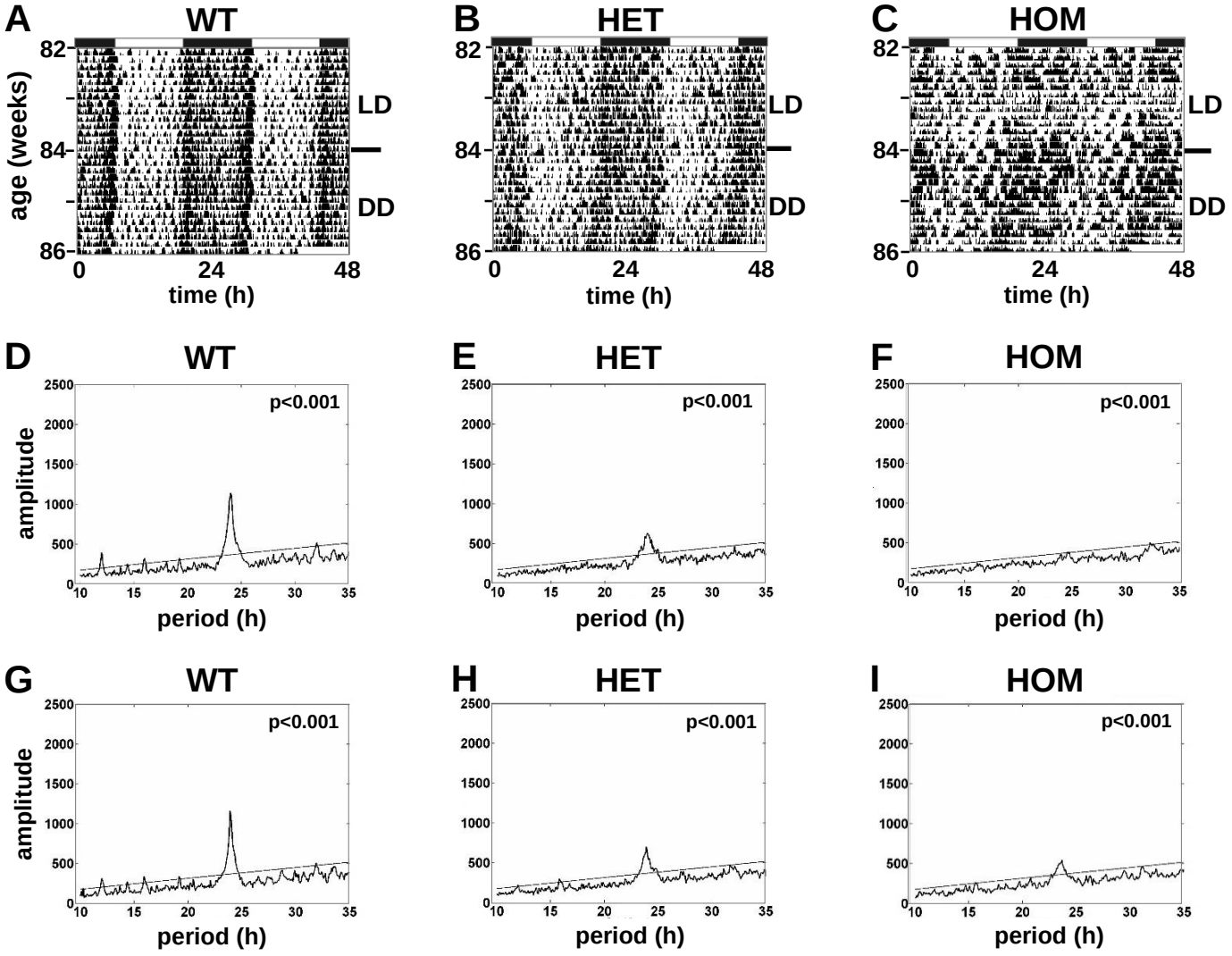
A
WT
B
HET
C
HOM
age (weeks)
82
84
86
LD
DD
0
24
48
time (h)
D
WT
E
HET
F
HOM
amplitude
p<0.001
2500
2000
1500
1000
500
0
10
15
20
25
30
35
period (h)
G
WT
H
HET
I
HOM

Figure 3

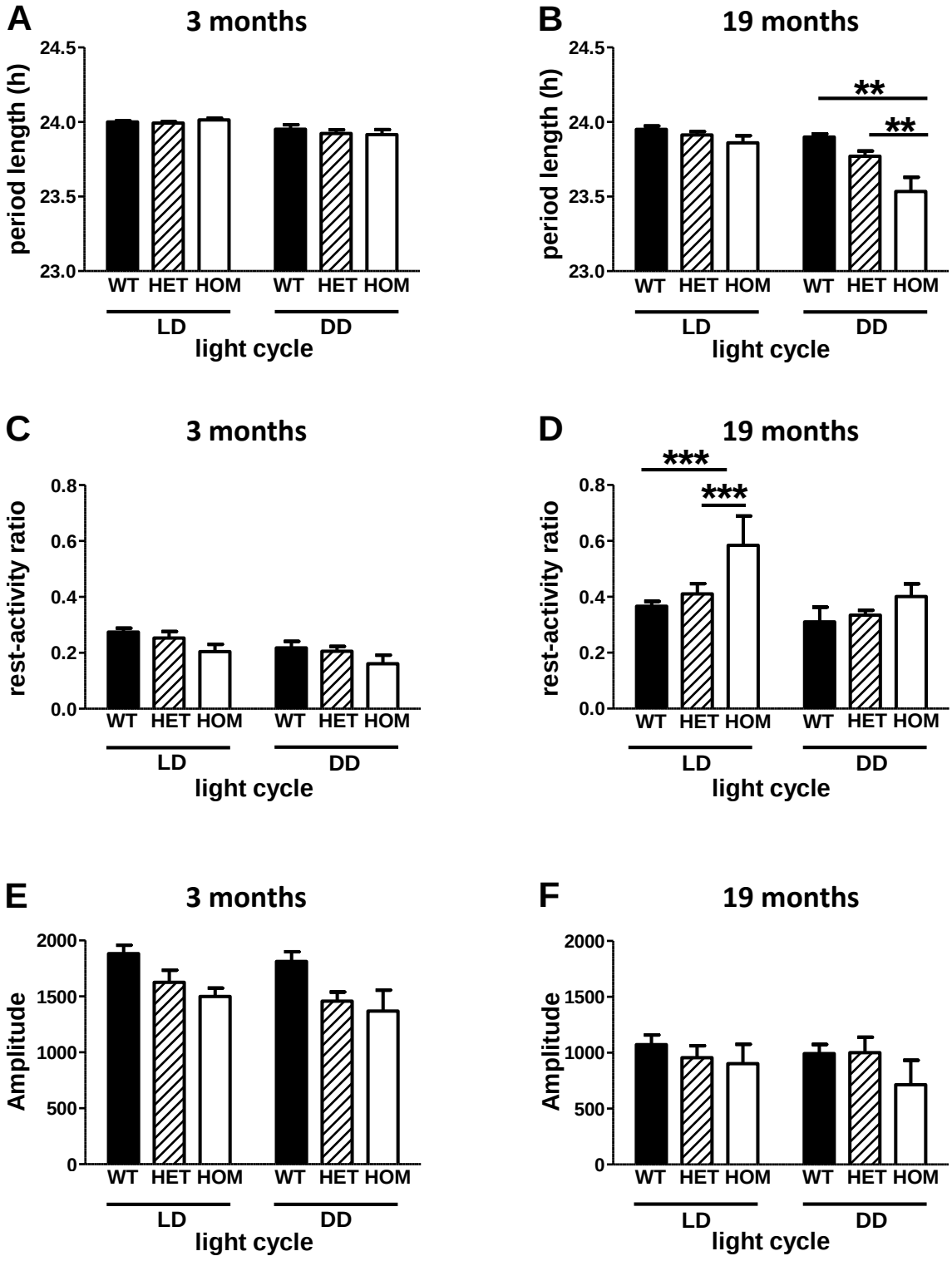
A
3 months
period length (h)
24.5
24.0
23.5
23.0
WT HET HOM WT HET HOM
LD
DD
light cycle
B
19 months
period length (h)
**
**
C
3 months
rest-activity ratio
0.8
0.6
0.4
0.2
0.0
D
19 months
***
***
E
3 months
Amplitude
2000
1500
1000
500
0
F
19 months

Figure 4

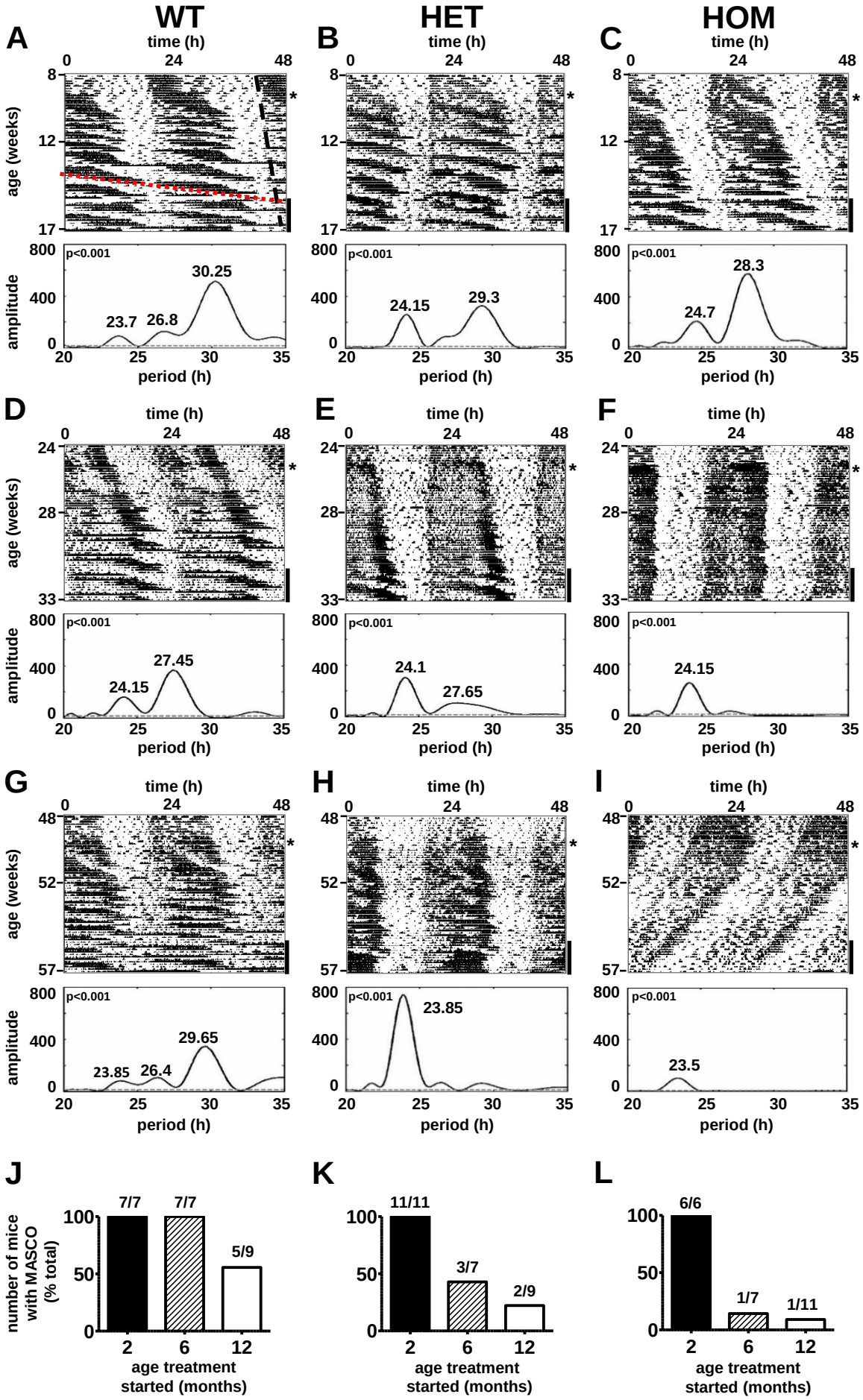
WT
HET
HOM
A
B
C
D
E
F
G
H
I
time (h)
0
24
48
age (weeks)
8
12
17
28
33
52
57
*
amplitude
800
400
0
p<0.001
30.25
23.7
26.8
24.15
29.3
28.3
24.7
27.45
24.1
27.65
29.65
23.85
26.4
23.5
20
25
30
35
period (h)
J
K
L
number of mice with MASCO (% total)
100
50
0
7/7
7/7
5/9
11/11
3/7
2/9
6/6
1/7
1/11
2
6
12
age treatment started (months)

Figure 5

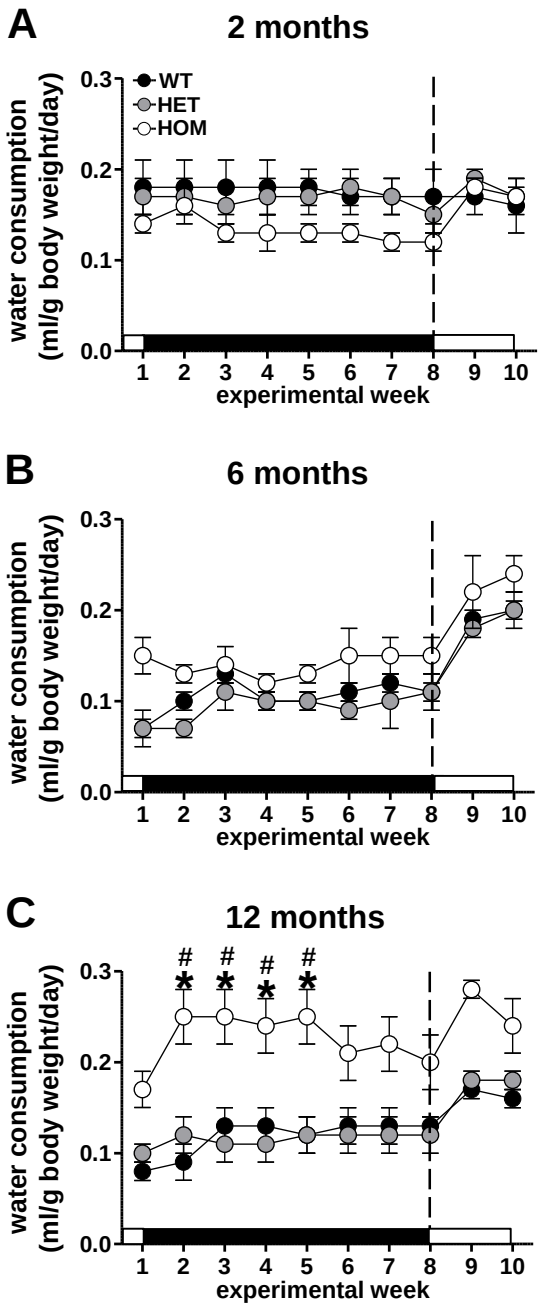
A
2 months
WT
HET
HOM
water consumption
(ml/g body weight/day)
0.3
0.2
0.1
0.0
1 2 3 4 5 6 7 8 9 10
experimental week
B
6 months
water consumption
(ml/g body weight/day)
0.3
0.2
0.1
0.0
1 2 3 4 5 6 7 8 9 10
experimental week
C
12 months
# # # #
* * * *
water consumption
(ml/g body weight/day)
0.3
0.2
0.1
0.0
1 2 3 4 5 6 7 8 9 10
experimental week

Figure 6

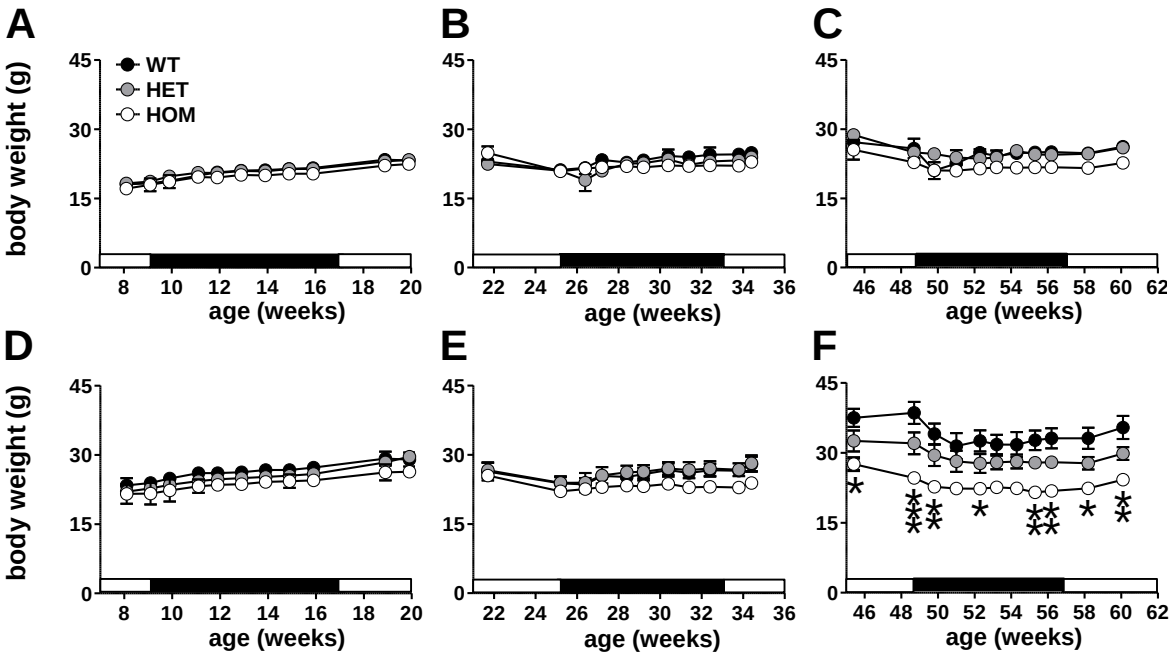
A
B
C
D
E
F
body weight (g)
age (weeks)
WT
HET
HOM
0
15
30
45
8
10
12
14
16
18
20
22
24
26
28
30
32
34
36
46
48
50
52
54
56
58
60
62

Figure 7

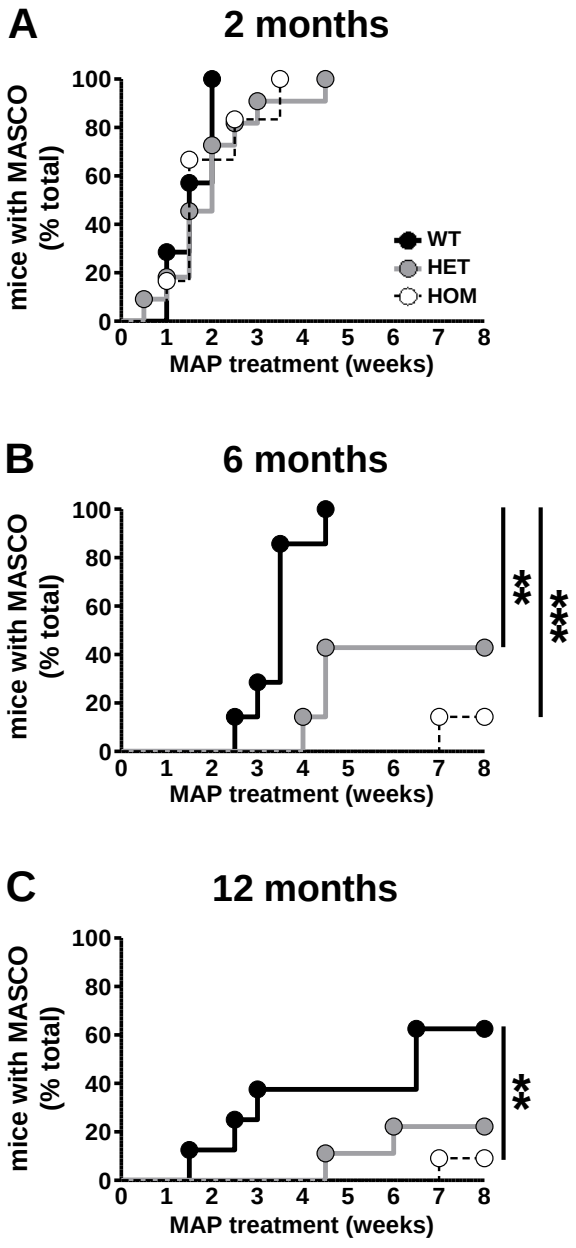
A
2 months
mice with MASCO (% total)
MAP treatment (weeks)
WT
HET
HOM
B
6 months
mice with MASCO (% total)
MAP treatment (weeks)
**
***
C
12 months
mice with MASCO (% total)
MAP treatment (weeks)
**

Figure 8

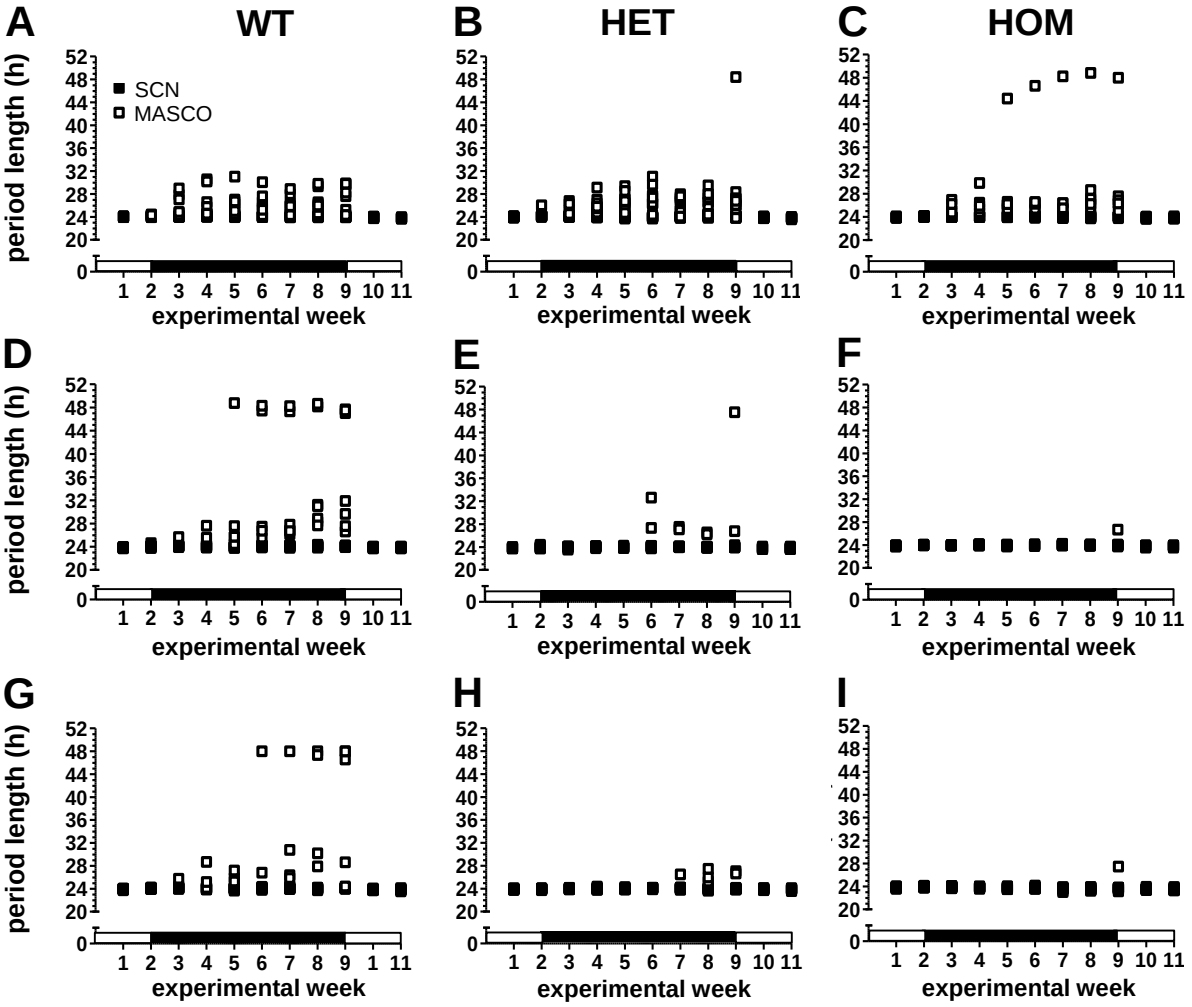
A
WT
B
HET
C
HOM
D
E
F
G
H
I
period length (h)
SCN
MASCO
experimental week
0
20
24
28
32
36
40
44
48
52
1 2 3 4 5 6 7 8 9 10 11

Figure 9

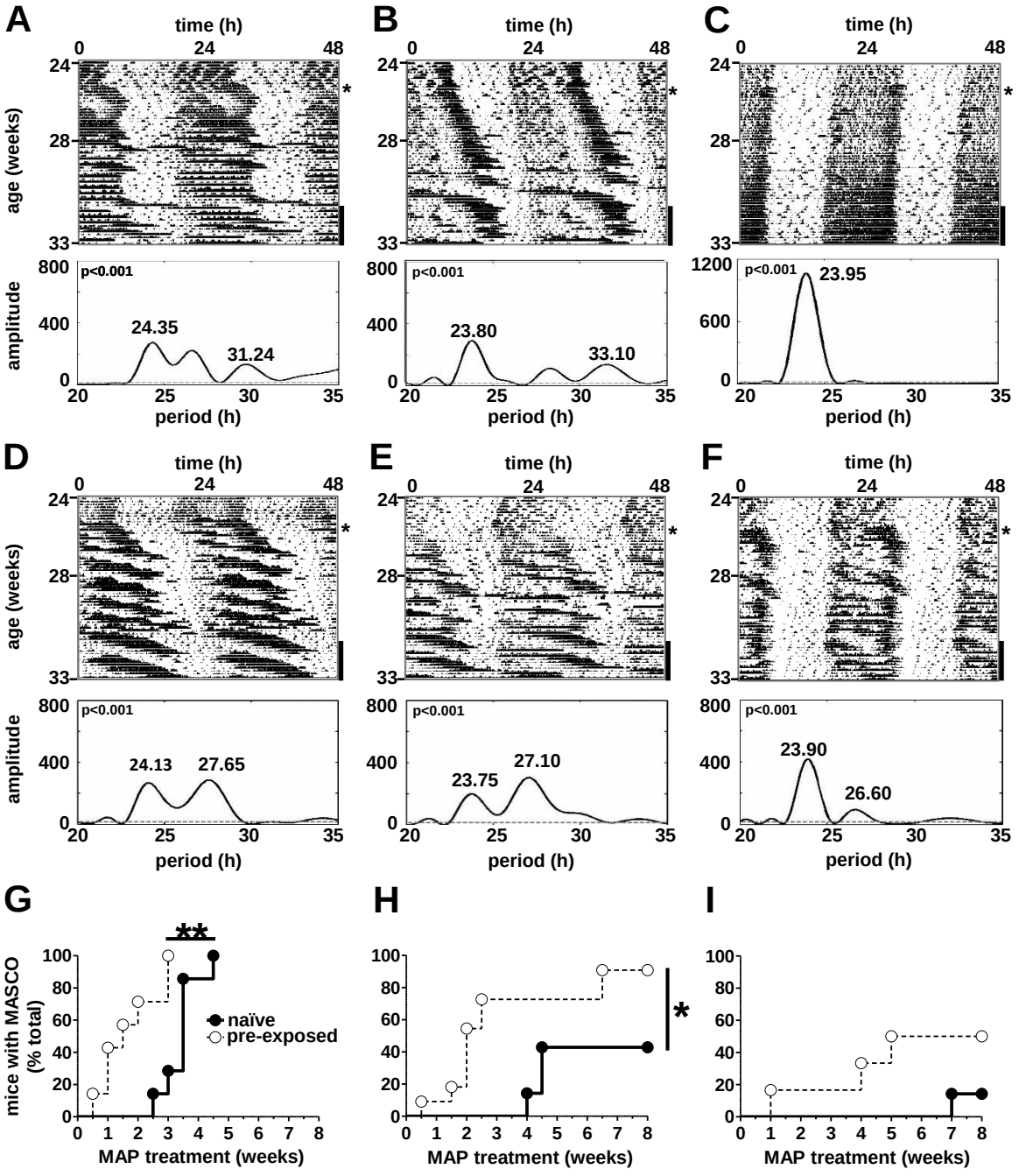
A
B
C
D
E
F
G
H
I
time (h)
0
24
48
age (weeks)
24
28
33
*
amplitude
800
400
0
p<0.001
24.35
31.24
23.80
33.10
1200
600
23.95
24.13
27.65
23.75
27.10
23.90
26.60
20
25
30
35
period (h)
mice with MASCO (% total)
100
80
60
40
20
0
**
naïve
pre-exposed
1
2
3
4
5
6
7
8
MAP treatment (weeks)

Supplementary Figure 1

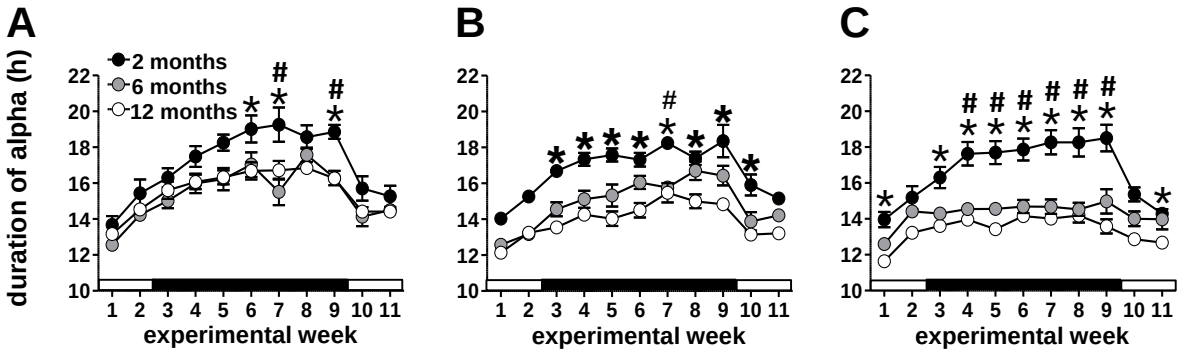

Supplementary Figure 2